Elucidation of the 14-3-3ζ interactome reveals critical roles of RNA splicing factors during adipogenesis

Yves Mugabo[1,2], Mina Sadeghi[1,2], Nancy N. Fang[3,4], Thibault Mayor[3], Gareth E. Lim[1,2,*]

[1]CRCHUM, Montréal, QC H2X 029, Canada
[2]Department of Medicine, Université de Montréal, Montréal, QC H3T 1J4, Canada
[3]Department of Biochemistry and Molecular Biology, University of British Columbia. Vancouver, Canada
[4]Present Address: Department of Medical Genetics, Harvard Medical School, Boston, USA.

***Corresponding author:**

Gareth E. Lim, Ph.D.
CRCHUM
Tour Viger, Rm 08.482
900 Rue St. Denis
Montréal, QC H2X 029
Canada
E-mail: gareth.lim@umontreal.ca
Tel: +1-514-890-8000 ext 12927

Running title: Identification of novel adipogenic factors in the 14-3-3ζ interactome

Key words: 14-3-3, adipocyte, RNA splicing, proteomics, adipogenesis, interactome

Abstract

Adipogenesis is facilitated by a complex signaling network requiring strict temporal and spatial organization of effector molecules. Molecular scaffolds, such as 14-3-3 proteins, coordinate such events, and we have previously identified 14-3-3ζ as an essential scaffold in adipocyte differentiation. The interactome of 14-3-3ζ is large and diverse, and it is possible that novel adipogenic factors may be present within it. Mouse embryonic fibroblasts from mice over-expressing a TAP-epitope-tagged 14-3-3ζ molecule were generated, and following the induction of adipogenesis, TAP-14-3-3ζ complexes were purified, followed by mass spectrometry analysis to determine the 14-3-3ζ interactome. Over 100 proteins were identified as being unique to adipocyte differentiation, of which 56 were novel interacting partners. Previously established regulators of adipogenesis (ie, Ptrf/Cavin1 and Phb2) were found within the 14-3-3ζ interactome, confirming the ability of this approach to identify regulators of adipocyte differentiation. An enrichment of proteins in the interactome related to RNA metabolism, processing, and splicing was identified, and analysis of transcriptomic data revealed that 14-3-3ζ depletion in 3T3-L1 cells affected the alternative splicing of mRNA during adipocyte differentiation. Of the RNA splicing factors within the 14-3-3ζ interactome, depletion of Hnrnpf, Hnrnpk, Ddx6, and Sfpq by siRNA revealed essential roles of these proteins in adipogenesis and their roles in the alternative splicing of *Lpin1*. In summary, novel adipogenic factors can be detected within the 14-3-3ζ interactome, and further characterization of additional proteins within the 14-3-3ζ interactome has the potential of identifying novel targets to block the expansion of adipose tissue mass that occurs in obesity.

1. Introduction

Central to the development of obesity are the increases in number and size of adipocytes according to nutrient availability (1,2). Despite various therapies to limit weight gain and promote weight loss, it is surprising that none specifically target the adipocyte to limit its expansion or growth (1,2). The complex transcriptional network and cellular processes that govern the differentiation of adipocyte progenitor cells contributes to the difficulty in targeting adipocytes therapeutically (1,2). Protein phosphorylation is a key post-translational modification that determines the activation state, subcellular localization, and stability of adipogenic regulators (3-7). Furthermore, phosphorylation status also determines their interactions with molecular scaffold proteins, which aid in the coordination of complex transcriptional networks (3,4) .

We previously identified the molecular scaffold, 14-3-3ζ, as a critical regulator of glucose homeostasis and adipogenesis (4,8,9). Specific to the adipocyte, systemic deletion of 14-3-3ζ in mice significantly reduced visceral adiposity and impaired adipocyte differentiation, whereas transgenic over-expression of 14-3-3ζ exacerbated high-fat diet induced obesity (4). The hedgehog transcription factor, Gli3, was identified as a critical downstream effector in 14-3-3ζ-mediated adipogenesis, but the diversity of proteins in the 14-3-3ζ interactome suggest the possibility that other interacting proteins or pathways parallel to Gli3 may be also involved.

Unbiased approaches, such as proteomics and transcriptomics, can lead to the discovery of novel factors that drive adipogenesis, in addition to providing insight into physiological pathways influenced by adipogenic regulators like 14-3-3ζ (4,10-15). All seven mammalian 14-3-3 isoforms have large, diverse interactomes (8,16-18), and they are dynamic and change in response to various stimuli (11-13,19). Thus, inducing pre-adipocytes to differentiate may permit the identification of novel differentiation-specific factors within the 14-3-3ζ interactome and reveal pathways and biological processes that are essential to the development of a mature adipocyte.

To elucidate the 14-3-3ζ interactome during adipogenesis, we employed a proteomic-based discovery approach. Herein, we report that previously established factors required for adipogenesis (ie, Ptrf/Cavin1 and Phb2) can be detected in the interactome, and novel factors, such as those involved in RNA splicing, are also enriched in the interactome during differentiation. To test for their roles in adipogenesis, siRNA knockdown approaches were used and revealed the requirement for RNA splicing factors, such as Hnrnpf, Sfpq, and Ddx6. Taken together these findings demonstrate the usefulness of examining the interactome of 14-3-3 proteins in the context of a physiological process, such as adipocyte differentiation, and highlight the ability to find novel

functional regulators through this approach. Understanding how the interactome is influenced by disease states, such as obesity, may lead to the identification of novel proteins that contribute to disease pathogenesis.

2. Material and methods

2.1 Generation of 14-3-3ζ^{TAP} MEFs and Cell culture

Embryos at e13.5 were harvested from pregnant transgenic mice over-expressing a TAP-epitope-tagged 14-3-3ζ molecule (4), and mouse embryonic fibroblasts (MEFs) were generated according to established protocols. 3T3-L1 cells (between passages 11-17) and mouse embryonic fibroblasts (MEFs) were maintained in 25mM glucose DMEM, supplemented with 10% newborn calf serum or fetal bovine serum (FBS), respectively, and 1% penicillin/streptomycin (ThermoFisher Scientific, Waltham, MA). Differentiation of MEFs and 3T3-L1 cells was induced with DMEM, supplemented with 10% FBS, 172 nM insulin, 500 μM IBMX, and 500 nM dexamethasone (MDI). Differentiation media for MEFs was further supplemented with rosiglitazone (Sigma-Aldrich, Oakville, ON, Canada). Following incubation with differentiation media for 2 days, media was replaced every two days with 25mM glucose DMEM, supplemented with 10% fetal bovine serum and 172 nM insulin. Differentiation was assessed by Oil Red-O incorporation (Sigma-Aldrich), as previously described (4).

2.2 Mass spectrometry

Equal amounts of cell lysates from undifferentiated and differentiated TAP-14-3-3ζ MEFs were subjected to an overnight incubation with IgG coupled to protein-G beads (ThermoFisher Scientific) in RIPA buffer. Bound proteins from each pull down were eluted with 1X SDS sample buffer without reducing agents and separated by SDS-PAGE prior to in-gel digestion (20). For each sample, peptides from three fractions (<50KDa, >50KDa, IgG bands) were then purified on C-18 stage tips (21) and analyzed using a LTQ-Orbitrap Velos (ThermoFisher Scientific) as previously described (22). Data were processed with Proteome Discoverer v. 1.2 (ThermoFisher Scientific) followed by a Mascot analysis (2.3.0, Matrix Science, Boston, MA) using the *Uniprot-Swissprot_mouse* protein database (05302013, 540261 protein sequences). Only proteins with at least two peptides (false positive discovery rate <=1%) in one of the two samples were retained. Two independent pull-downs were used for mass spectrometry and proteomic analysis. Proteins were analyzed with DAVID and String-Db to analyze proteins based their biological processes (23,24).

2.3 Analysis of differential exon usage

To understand how adipocyte differentiation and depletion of 14-3-3ζ affected alternative splicing of mRNA, differential exon usage via DEXSeq was used as a surrogate measurement (25). Our previous transcriptomic data [GSE60745] (26) were aligned to the mouse genome (Ensembl NCBIM37) via Tophat (v. 2.1.1), and the number of reads mapping to a particular exon were compared to the total number of exons in a given gene (25). A false discovery rate (FDR) of 0.05 was used to filter results. This dataset was also analyzed to examined how depletion of 14-3-3ζ or differentiation affects the expression profile of target genes. Genes identified by DEXSeq were subjected to gene ontology analysis to categorize genes by biological function (27). Alternatively, analysis of *Lpin1* splicing was performed by RT-PCR, as described previously (28). PCR products were resolved on an agarose gel, followed by densitometric analysis of splice variants by ImageJ (29).

2.4 siRNA-mediated knockdown, RNA isolation and quantitative PCR

3T3-L1 cells were seeded at a density of 75,000 per well prior to transfection with control siRNA or target-specific Silencer Select siRNAs (ThermoFisher Scientific). Transfection was performed using Lipofectamine RNAimax, as per manufacturer instructions (ThermoFisher Scientific), at a final siRNA concentration of 20 μM per well. RNA was isolated from 3T3-L1 adipocytes or MEFs with the RNEasy kit (Qiagen, Mississauga, ON, Canada). Synthesis of cDNA was performed with the qScript cDNA Synthesis kit (Quanta Biosciences, Gaithersburg, MD), and transcript levels were measured with SYBR green chemistry or Taqman assays on a QuantStudio 6-flex Real-time PCR System (ThermoFisher Scientific). Primer sequences are available on request. All data were normalized to HPRT by the $2^{-\Delta Ct}$ method, as previously described (4,9,30). Confirmation that knockdown of 14-3-3ζ has no effect of global RNA transcription was determined using the Click-iT RNA Alexa 488 imaging kit, as per manufacturer instructions (Thermo Scientific).

2.5 Statistical Analysis

All data were analyzed by one- or two-way ANOVA, followed by appropriate post-hoc tests, or by Student's t-test. Data were considered significant when $p<0.05$.

3. Results

3.1 Generation of TAP-14-3-3ζ mouse embryonic fibroblasts (MEFs)

To examine how adipocyte differentiation influences the 14-3-3ζ interactome, we generated mouse embryonic fibroblasts (MEFs) derived from transgenic mice that moderately over-express a TAP-epitope tagged human 14-3-3ζ molecule (TAP-14-3-3ζ) (4,31) (Figure 1A). This approach was chosen to circumvent the variability in the expression of transiently expressed proteins and increased specificity of protein purification with epitope-tagged proteins (32,33). Differentiation of MEFs was induced with an established adipogenic cocktail (insulin, dexamethasone, and IBMX), supplemented with rosiglitazone (Figure 1A,B). Differentiation into adipocytes was confirmed by Oil Red-O staining and *Pparg* mRNA expression (Figure 1B,C).

3.2 Differentiation of TAP-14-3-3ζ MEFs results in distinct changes in the interactome of 14-3-3ζ

Although we previously identified the hedgehog signaling effector, Gli3, as a downstream regulator of 14-3-3ζ-dependent adipogenesis (4), we hypothesized that 14-3-3ζ may control other parallel processes underlying adipocyte differentiation. This is due in part to the large, diverse interactomes of 14-3-3 proteins (8,16-18). Thus, we utilized affinity proteomics to identify interacting proteins that associate with 14-3-3ζ during adipocyte differentiation (Figure 1A). The interactome of 14-3-3ζ at 24 hours post-induction was examined because key signaling events underlying murine adipocyte differentiation occur during the first 24-48 hours (2,4,34). Over 100 proteins were identified by mass spectrometry as 14-3-3ζ interacting proteins (Table 1). Of these proteins, 56 have not been previously reported to interact with any member of the 14-3-3 protein family (Table 2) (17). 14-3-3ζ itself was found equally enriched in both samples, demonstrating equal pull-down efficiency (data not shown). An enrichment of differentiation-dependent 14-3-3ζ-interacting proteins associated with RNA splicing, translation, protein transport, and nucleic acid transport were detected using gene ontology to define their biological processes (23,24) (Table 3). Thus, these proteomic data demonstrate the dynamic nature of the 14-3-3ζ interactome and suggest that 14-3-3ζ may regulate multiple processes required for adipocyte differentiation through its interactions.

3.3 Regulation of mRNA processing by 14-3-3ζ

Using our previous transcriptomic analysis of differentiating 3T3-L1 cells (26), we re-analyzed the effects of differentiation and 14-3-3ζ depletion on RNA processing. Differential exon usage (DEXSeq) was used as a

surrogate measure of alternative splicing of mRNA (Figure 2A) (25). Any changes in splice variant levels were not due to global effects of 14-3-3ζ depletion on RNA transcription, as no gross differences in the incorporation of a uracil analog were detected (Figure 2B). Comparison of genes that displayed differential exon usage at 24 and 48 hours post differentiation revealed that 163 and 172 genes, respectively, that were unique to each time point (Figure 2C). Gene ontology analysis revealed that at each time point, distinct groups of genes were alternatively spliced (Table 4). The use of this approach to detect genes with differential exon usage was validated by the ability to detect *Pparg* variants after 48 hours of differentiation (Figure S1) (35). The effect of 14-3-3ζ depletion was assessed at each time point, and 78, 37, and 36 genes were affected following 14-3-3ζ knockdown at 0, 24, and 48 hours, respectively, after the induction of differentiation (Figure 2D). However, only in undifferentiated 3T3-L1 cells could enrichments in genes associated with macromolecular complex assembly (GO:0065003, $p=3.44 \times 10^{-3}$), macromolecular complex subunit organization (GO:0043933, $p= 7.56 \times 10^{-4}$), and regulation of biological quality (GO:0065008, $p=9.51 \times 10^{-3}$) be detected by gene ontology analysis. Collectively, these data demonstrate that adipogenesis promotes the alternative splicing of genes and this process can be influenced by 14-3-3ζ.

3.4 Identification of known and novel regulators of adipocyte differentiation

Within the 14-3-3ζ interactome, we were able to detect proteins with known roles in adipogenesis, such as Ptrf/Cavin1 and prohibitin-2 (Phb2) (36-40) and confirmed their roles in adipocyte differentiation (Figure 3). This confirmed that known regulators of adipogenesis can be detected within the 14-3-3ζ interactome and suggested the possibility that novel factors could be identified. Additional proteins in the 14-3-3ζ interactome, such as Fragile-X mental retardation protein-1 (Fmr1) and Rpn2, were also examined for their roles in adipogenesis, as they have previously been shown to be associated with obesity or weight gain (41,42). However, siRNA-mediated knockdown of either protein had no effect on 3T3-L1 differentiation, indicating that these proteins are not required for adipogenesis (Figure 3A-D), at least in this *in vitro* model system.

As proteins associated with RNA processing and splicing were highly enriched during differentiation (Table 3), we sought to examine contribution of RNA splicing factors to adipogenesis. Using siRNA in 3T3-L1 pre-adipocytes, 8 splicing factors, which were identified in our proteomic analysis of the 14-3-3ζ interactome (Table 1), were screened for their roles in 3T3-L1 adipogenesis. They were chosen by the number of connections exhibited within each cluster of proteins (Figure 1D) (24). Of note, mRNA levels of the chosen

splicing factors were generally unaffected by knockdown of 14-3-3ζ; however, some splicing factors were influenced by differentiation (Figure S2) (26). Transient knockdown of Ddx6, Sfpq, Hnrnpf, or Hnrnpk was sufficient to impair 3T3-L1 differentiation, as assessed by Oil Red-O incorporation (Figure 4). Closely related proteins with similar roles, such as Ddx1, Nono, Hnrnpm, and Syncrip/Hnrnpq were not required for 3T3-L1 adipogenesis (Figure 4B, C). Knockdown of Ddx6 or Hnrnpk by siRNA did not have an effect of *Pparg*, which suggests that these factors act downstream of the mRNA expression of this master transcription factor (Figure 4D). Other pro- or anti-adipogenic genes are alternatively spliced during adipocyte differentiation. For example, *Lpin1* mRNA is spliced to generate Lipin-1α and Lipin-1β, which have differential roles on adipogenesis (28). To examine the effect of depletion of 14-3-3ζ, Hnrnpf, Ddx6, Hnrnpk, and Sfpq on *Lpin1* splicing, 3T3-L1 cells were transiently transfected with siRNA, followed by the induction of differentiation. Gene silencing of all target genes was found to prevent the generation of the *Lpin-1*α variant during differentiation (Figure 4E, F). Collectively, these findings demonstrate that novel regulators of adipogenesis can be identified within the interactome of 14-3-3ζ and highlight the involvement of 14-3-3ζ in regulating the alternative splicing of mRNA.

4. Discussion

In the present study, affinity proteomics was used to determine how adipogenesis influences the interactome of 14-3-3ζ. Surprisingly, the interactome was dynamic, as differentiation altered the landscape of proteins that interact with 14-3-3ζ. This approach also permitted the identification of known adipogenic factors within the 14-3-3ζ interactome and revealed novel proteins that are required for adipocyte differentiation. An enrichment of proteins associated with RNA processing and splicing were detected, and the novel contributions of RNA splicing factors, such as Hnrnpf, Ddx6, and Sfpq, in adipogenesis were identified. The usefulness of this approach was also evident in the ability to identify process that may be regulated by 14-3-3ζ during adipocyte differentiation.

We previously identified an essential function of the hedgehog signaling effector Gli3 in 14-3-3ζ-regulated adipocyte differentiation (4). However, due to the large, diverse interactome of 14-3-3 proteins (10,13,16,17), we hypothesized that it is unlikely that one protein would be solely responsible for 14-3-3ζ-mediated adipogenesis. It is known that the interactomes of 14-3-3 proteins are dynamic and change in response to various stimuli (11-13,19). The functional significance of such changes in the interactome is not clear, but it suggests that 14-3-3 proteins may be regulating biological processes critical for adipocyte

development through their interactions. Using a gene onotology-based approach, we found that the 14-3-3ζ interactome is enriched with proteins involved in RNA binding and splicing during differentiation and confirms its contribution to the alternative splicing of mRNAs. As over 100 proteins were found to be unique to the14-3-3ζ interactome during adipocyte differentiation, it suggests that 14-3-3ζ could also regulate other cellular processes required for adipocyte development. For example, we detected an interaction of 14-3-3ζ with the mitochondrial regulator, Prohibitin-2 (Phb2), which others have shown to be essential for the expansion of mitochondria mass and mitochondrial function during adipogenesis (36-38). Further in-depth studies are required to assess whether 14-3-3ζ has regulatory roles in mitochondrial dynamics, but when taken together, it demonstrates the possibility of examining the contributions of interacting partners to reveal novel biological processes required for adipocyte differentiation.

Through the use of a functional siRNA screen, we identified novel roles of various RNA splicing factors, namely Hnrpnf, Hnrnpk, Ddx6, and Sfpq, in adipocyte differentiation. Sfpq belongs to the Drosophila behavior/human splicing (DHBS) protein family and is required for transcriptional regulation (43,44). Although a recent study by Wang and colleagues found no effect of forced overexpression of Nono and Sfpq on adipogenesis (45), we report that Sfpq depletion impairs adipocyte differentiation. DHBS proteins may exhibit redundant, compensatory functions (46), but given that only Sfpq depletion impaired 3T3-L1 adipogenesis, it suggests specific protein-protein or protein-nucleic acid interactions occur may with each DHBS member in the context of differentiation (44). We were also able to detect novel adipogenic roles of Hnrnpf and Hnrnpk, members of the heterogeneous nuclear ribonucleoproteins (Hnrnps) which facilitate mRNA splicing (47,48). Alternative splicing of mRNA is critical for maintaining genetic diversity and cell identity, in addition to the expression of key factors required for differentiation (49,50). Specific to adipogenesis, differential promoter usage and alternative splicing are required for the expression of the canonical adipogenic transcription factor Pparγ (51-53). Other regulatory factors are also formed from alternative splicing, including nCOR1 and Lipin1 (54,55). Future studies are required to determine whether 14-3-3ζ directly binds to these splicing factors and how it regulates their splicing activity to generate essential adipogenic factors.

Protein abundance of 14-3-3ζ and other isoforms is increased in visceral adipose tissue from obese individuals (56,57), and we have previously reported that systemic over-expression of 14-3-3ζ in mice is sufficient to potentiate weight gain and fat mass in mice fed a high-fat diet (4). With respect to the pancreatic β-cell, single cell transcriptomic analysis revealed higher mRNA expression of *YWHAZ* in β-cells from subjects

with type 2 diabetes (58), and we have found that systemic over-expression of 14-3-3ζ was sufficient to reduce β-cell secretory function in mice (9). The exact mechanisms owing to how changes in 14-3-3ζ function affects the development of obesity or β-cell dysfunction are not known, but In-depth examination of the interactome in the context of both conditions may yield novel biological insight as to how 14-3-3ζ influences their development. This approach has already been useful in understanding how changes in 14-3-3ε or 14-3-3σ expression can lead to the development of various forms of cancer and the identification of novel therapeutic targets (19,59-61).

In conclusion, this study provides compelling evidence demonstrating the usefulness of elucidating the interactome of 14-3-3ζ as a means to identify novel factors required for adipogenesis. Additionally, a systematic investigation of interacting partners may also provide insight as to which physiological processes are essential for 14-3-3ζ-mediated adipocyte differentiation. Lastly, deciphering how various disease states influence the interactome of 14-3-3 proteins may also aid in the discovery of novel therapeutic targets for the treatment of chronic diseases, such as obesity and type 2 diabetes.

5. Acknowledgements

This work was supported by a CIHR Project grant (PJT-153144) to GEL. Some of this work was initiated by GEL when he was a JDRF- and Canadian Diabetes Association-supported postdoctoral fellow in the lab of Dr. James D. Johnson (University of British Columbia, Vancouver, BC, Canada). The authors would like to thank François Harvey in the Bioinformatics platform at the CRCHUM for bioinformatics support, as well as Dr. Johnson for critical reading of this manuscript.

6. Authors contribution

Y.M performed experiments, analyzed data, and wrote and reviewed the manuscript. MS and NNF performed experiments and analyzed data. TM designed parts of the study and reviewed the manuscript. GEL performed experiments, analyzed data, wrote the manuscript, and is responsible for the integrity of this work.

7. References

1. Rosen, E. D., and MacDougald, O. A. (2006) Adipocyte differentiation from the inside out. *Nat Rev Mol Cell Biol* **7**, 885-896

2. Cristancho, A. G., and Lazar, M. A. (2011) Forming functional fat: a growing understanding of adipocyte differentiation. *Nature Rev Mol Endocrinol* **12**, 722-734

3. Scott, J. D., and Pawson, T. (2009) Cell signaling in space and time: where proteins come together and when they're apart. *Science* **326**, 1220-1224

4. Lim, G. E., Albrecht, T., Piske, M., Sarai, K., Lee, J. T., Ramshaw, H. S., Sinha, S., Guthridge, M. A., Acker-Palmer, A., Lopez, A. F., Clee, S. M., Nislow, C., and Johnson, J. D. (2015) 14-3-3zeta coordinates adipogenesis of visceral fat. *Nat Commun* **6**, 7671

5. Brunet, A., Kanai, F., Stehn, J., Xu, J., Sarbassova, D., Frangioni, J. V., Dalal, S. N., DeCaprio, J. A., Greenberg, M. E., and Yaffe, M. B. (2002) 14-3-3 transits to the nucleus and participates in dynamic nucleocytoplasmic transport. *The Journal of cell biology* **156**, 817-828

6. Nakae, J., Kitamura, T., Kitamura, Y., Biggs, W. H., 3rd, Arden, K. C., and Accili, D. (2003) The forkhead transcription factor Foxo1 regulates adipocyte differentiation. *Dev cell* **4**, 119-129

7. Feige, J. N., and Auwerx, J. (2007) Transcriptional coregulators in the control of energy homeostasis. *Trends Cell Biol* **17**, 292-301

8. Lim, G. E., and Johnson, J. D. (2016) 14-3-3zeta: A numbers game in adipocyte function? *Adipocyte* **5**, 232-237

9. Lim, G. E., Piske, M., Lulo, J. E., Ramshaw, H. S., Lopez, A. F., and Johnson, J. D. (2016) Ywhaz/14-3-3zeta deletion improves glucose tolerance through a GLP-1-dependent mechanism. *Endocrinology*, en20161016

10. Pozuelo Rubio, M., Geraghty, K. M., Wong, B. H., Wood, N. T., Campbell, D. G., Morrice, N., and Mackintosh, C. (2004) 14-3-3-affinity purification of over 200 human phosphoproteins reveals new links to regulation of cellular metabolism, proliferation and trafficking. *Biochem J* **379**, 395-408

11. Chen, S., Synowsky, S., Tinti, M., and Mackintosh, C. (2011) The capture of phosphoproteins by 14-3-3 proteins mediates actions of insulin. *Trends Endocrinol Metab* **22**, 429-436

12. Ohman, T., Soderholm, S., Hintsanen, P., Valimaki, E., Lietzen, N., MacKintosh, C., Aittokallio, T., Matikainen, S., and Nyman, T. A. (2014) Phosphoproteomics combined with quantitative 14-3-3-affinity capture identifies SIRT1 and RAI as novel regulators of cytosolic double-stranded RNA recognition pathway. *Mol Cell Proteomics* **13**, 2604-2617

13. Pozuelo-Rubio, M. (2010) Proteomic and biochemical analysis of 14-3-3-binding proteins during C2-ceramide-induced apoptosis. *FEBS J* **277**, 3321-3342

14. Siersbaek, R., Nielsen, R., John, S., Sung, M. H., Baek, S., Loft, A., Hager, G. L., and Mandrup, S. (2011) Extensive chromatin remodelling and establishment of transcription factor 'hotspots' during early adipogenesis. *EMBO J* **30**, 1459-1472

15. Siersbaek, R., Rabiee, A., Nielsen, R., Sidoli, S., Traynor, S., Loft, A., Poulsen, L. L., Rogowska-Wrzesinska, A., Jensen, O. N., and Mandrup, S. (2014) Transcription Factor Cooperativity in Early Adipogenic Hotspots and Super-Enhancers. *Cell reports* **7**, 1443-1455

16. Johnson, C., Crowther, S., Stafford, M. J., Campbell, D. G., Toth, R., and MacKintosh, C. (2010) Bioinformatic and experimental survey of 14-3-3-binding sites. *Biochem J* **427**, 69-78

17. Johnson, C., Tinti, M., Wood, N. T., Campbell, D. G., Toth, R., Dubois, F., Geraghty, K. M., Wong, B. H., Brown, L. J., Tyler, J., Gernez, A., Chen, S., Synowsky, S., and MacKintosh, C. (2011) Visualization and biochemical analyses of the emerging mammalian 14-3-3-phosphoproteome. *Mol Cell Proteomics* **10**, M110 005751

18. Mackintosh, C. (2004) Dynamic interactions between 14-3-3 proteins and phosphoproteins regulate diverse cellular processes. *Biochem J* **381**, 329-342

19. Weerasekara, V. K., Panek, D. J., Broadbent, D. G., Mortenson, J. B., Mathis, A. D., Logan, G. N., Prince, J. T., Thomson, D. M., Thompson, J. W., and Andersen, J. L. (2014) Metabolic-stress-induced rearrangement of the 14-3-3zeta interactome promotes autophagy via a ULK1- and AMPK-regulated 14-3-3zeta interaction with phosphorylated Atg9. *Mol Cell Biol* **34**, 4379-4388

20. Shevchenko, A., Chernushevich, I., Wilm, M., and Mann, M. (2000) De Novo peptide sequencing by nanoelectrospray tandem mass spectrometry using triple quadrupole and quadrupole/time-of-flight instruments. *Methods Mol Biol* **146**, 1-16

21. Rappsilber, J., Mann, M., and Ishihama, Y. (2007) Protocol for micro-purification, enrichment, pre-fractionation and storage of peptides for proteomics using StageTips. *Nat Protoc* **2**, 1896-1906

22. Ng, A. H., Fang, N. N., Comyn, S. A., Gsponer, J., and Mayor, T. (2013) System-Wide Analysis Reveals Intrinsically Disordered Proteins are Prone to Ubiquitylation after Misfolding Stress. *Mol Cell Proteomics*

23. Huang da, W., Sherman, B. T., and Lempicki, R. A. (2009) Systematic and integrative analysis of large gene lists using DAVID bioinformatics resources. *Nat Protoc* **4**, 44-57

24. Szklarczyk, D., Morris, J. H., Cook, H., Kuhn, M., Wyder, S., Simonovic, M., Santos, A., Doncheva, N. T., Roth, A., Bork, P., Jensen, L. J., and von Mering, C. (2017) The STRING database in 2017: quality-controlled protein-protein association networks, made broadly accessible. *Nucleic Acids Res* **45**, D362-D368

25. Anders, S., Reyes, A., and Huber, W. (2012) Detecting differential usage of exons from RNA-seq data. *Genome Res* **22**, 2008-2017

26. Lim, G. E., ; Johnson, J.D. (2015) 14-3-3ζ controls adipocyte progenitor cell cycle and differentiation via Gli3-dependent p27Kip expression. *Gene Expression Omnibus (GEO)* **GSE60745**

27. Carbon, S., Ireland, A., Mungall, C. J., Shu, S., Marshall, B., Lewis, S., Ami, G. O. H., and Web Presence Working, G. (2009) AmiGO: online access to ontology and annotation data. *Bioinformatics* **25**, 288-289

28. Peterfy, M., Phan, J., and Reue, K. (2005) Alternatively spliced lipin isoforms exhibit distinct expression pattern, subcellular localization, and role in adipogenesis. *J Biol Chem* **280**, 32883-32889

29. Schneider, C. A., Rasband, W. S., and Eliceiri, K. W. (2012) NIH Image to ImageJ: 25 years of image analysis. *Nature methods* **9**, 671-675

30. Lim, G. E., Piske, M., and Johnson, J. D. (2013) 14-3-3 proteins are essential signalling hubs for beta cell survival. *Diabetologia* **56**, 825-837

31. Angrand, P. O., Segura, I., Volkel, P., Ghidelli, S., Terry, R., Brajenovic, M., Vintersten, K., Klein, R., Superti-Furga, G., Drewes, G., Kuster, B., Bouwmeester, T., and Acker-Palmer, A. (2006) Transgenic mouse proteomics identifies new 14-3-3-associated proteins involved in cytoskeletal rearrangements and cell signaling. *Mol Cell Proteomics* **5**, 2211-2227

32. Li, Y. (2010) Commonly used tag combinations for tandem affinity purification. *Biotechnol Appl Biochem* **55**, 73-83

33. Williamson, M. P., and Sutcliffe, M. J. (2010) Protein-protein interactions. *Biochem Soc Trans* **38**, 875-878

34. Yeh, W. C., Cao, Z., Classon, M., and McKnight, S. L. (1995) Cascade regulation of terminal adipocyte differentiation by three members of the C/EBP family of leucine zipper proteins. *Genes Dev* **9**, 168-181

35. Fajas, L., Auboeuf, D., Raspe, E., Schoonjans, K., Lefebvre, A. M., Saladin, R., Najib, J., Laville, M., Fruchart, J. C., Deeb, S., Vidal-Puig, A., Flier, J., Briggs, M. R., Staels, B., Vidal, H., and Auwerx, J. (1997) The organization, promoter analysis, and expression of the human PPARgamma gene. *J Biol Chem* **272**, 18779-18789

36. Liu, D., Lin, Y., Kang, T., Huang, B., Xu, W., Garcia-Barrio, M., Olatinwo, M., Matthews, R., Chen, Y. E., and Thompson, W. E. (2012) Mitochondrial dysfunction and adipogenic reduction by prohibitin silencing in 3T3-L1 cells. *PloS one* **7**, e34315

37. Ande, S. R., Nguyen, K. H., Padilla-Meier, G. P., Wahida, W., Nyomba, B. L., and Mishra, S. (2014) Prohibitin overexpression in adipocytes induces mitochondrial biogenesis, leads to obesity development, and affects glucose homeostasis in a sex-specific manner. *Diabetes* **63**, 3734-3741

38. Ande, S. R., Xu, Z., Gu, Y., and Mishra, S. (2012) Prohibitin has an important role in adipocyte differentiation. *Int J Obes (Lond)* **36**, 1236-1244

39. Ding, S. Y., Lee, M. J., Summer, R., Liu, L., Fried, S. K., and Pilch, P. F. (2014) Pleiotropic effects of cavin-1 deficiency on lipid metabolism. *J Biol Chem* **289**, 8473-8483

40. Perez-Diaz, S., Johnson, L. A., DeKroon, R. M., Moreno-Navarrete, J. M., Alzate, O., Fernandez-Real, J. M., Maeda, N., and Arbones-Mainar, J. M. (2014) Polymerase I and transcript release factor (PTRF) regulates adipocyte differentiation and determines adipose tissue expandability. *FASEB J* **28**, 3769-3779

41. McLennan, Y., Polussa, J., Tassone, F., and Hagerman, R. (2011) Fragile x syndrome. *Current genomics* **12**, 216-224

42. Brasaemle, D. L., Dolios, G., Shapiro, L., and Wang, R. (2004) Proteomic analysis of proteins associated with lipid droplets of basal and lipolytically stimulated 3T3-L1 adipocytes. *J Biol Chem* **279**, 46835-46842

43. Knott, G. J., Bond, C. S., and Fox, A. H. (2016) The DBHS proteins SFPQ, NONO and PSPC1: a multipurpose molecular scaffold. *Nucleic Acids Res* **44**, 3989-4004

44. Kowalska, E., Ripperger, J. A., Hoegger, D. C., Bruegger, P., Buch, T., Birchler, T., Mueller, A., Albrecht, U., Contaldo, C., and Brown, S. A. (2013) NONO couples the circadian clock to the cell cycle. *Proc Natl Acad Sci U S A* **110**, 1592-1599

45. Wang, J., Rajbhandari, P., Damianov, A., Han, A., Sallam, T., Waki, H., Villanueva, C. J., Lee, S. D., Nielsen, R., Mandrup, S., Reue, K., Young, S. G., Whitelegge, J., Saez, E., Black, D. L., and Tontonoz, P. (2017) RNA-binding protein PSPC1 promotes the differentiation-dependent nuclear export of adipocyte RNAs. *J Clin Invest* **127**, 987-1004

46. Li, S., Li, Z., Shu, F. J., Xiong, H., Phillips, A. C., and Dynan, W. S. (2014) Double-strand break repair deficiency in NONO knockout murine embryonic fibroblasts and compensation by spontaneous upregulation of the PSPC1 paralog. *Nucleic Acids Res* **42**, 9771-9780

47. Chaudhury, A., Chander, P., and Howe, P. H. (2010) Heterogeneous nuclear ribonucleoproteins (hnRNPs) in cellular processes: Focus on hnRNP E1's multifunctional regulatory roles. *Rna* **16**, 1449-1462

48. Dreyfuss, G., Kim, V. N., and Kataoka, N. (2002) Messenger-RNA-binding proteins and the messages they carry. *Nat Rev Mol Cell Biol* **3**, 195-205

49. Nilsen, T. W., and Graveley, B. R. (2010) Expansion of the eukaryotic proteome by alternative splicing. *Nature* **463**, 457-463

50. Lin, J. C. (2015) Impacts of Alternative Splicing Events on the Differentiation of Adipocytes. *International journal of molecular sciences* **16**, 22169-22189

51. McClelland, S., Shrivastava, R., and Medh, J. D. (2009) Regulation of Translational Efficiency by Disparate 5' UTRs of PPARgamma Splice Variants. *PPAR Res* **2009**, 193413

52. Zhu, Y., Qi, C., Korenberg, J. R., Chen, X. N., Noya, D., Rao, M. S., and Reddy, J. K. (1995) Structural organization of mouse peroxisome proliferator-activated receptor gamma (mPPAR gamma) gene: alternative promoter use and different splicing yield two mPPAR gamma isoforms. *Proc Natl Acad Sci U S A* **92**, 7921-7925

53. Tontonoz, P., Hu, E., Graves, R. A., Budavari, A. I., and Spiegelman, B. M. (1994) mPPAR gamma 2: tissue-specific regulator of an adipocyte enhancer. *Genes Dev* **8**, 1224-1234

54. Li, H., Cheng, Y., Wu, W., Liu, Y., Wei, N., Feng, X., Xie, Z., and Feng, Y. (2014) SRSF10 regulates alternative splicing and is required for adipocyte differentiation. *Mol Cell Biol* **34**, 2198-2207

55. Mei, B., Zhao, L., Chen, L., and Sul, H. S. (2002) Only the large soluble form of preadipocyte factor-1 (Pref-1), but not the small soluble and membrane forms, inhibits adipocyte differentiation: role of alternative splicing. *Biochem J* **364**, 137-144

56. Capobianco, V., Nardelli, C., Ferrigno, M., Iaffaldano, L., Pilone, V., Forestieri, P., Zambrano, N., and Sacchetti, L. (2012) miRNA and Protein Expression Profiles of Visceral Adipose Tissue Reveal miR-141/YWHAG and miR-520e/RAB11A as Two Potential miRNA/Protein Target Pairs Associated with Severe Obesity. *J Prot Res* **11**, 3358-3369

57. Insenser, M., Montes-Nieto, R., Vilarrasa, N., Lecube, A., Simo, R., Vendrell, J., and Escobar-Morreale, H. F. (2012) A nontargeted proteomic approach to the study of visceral and subcutaneous adipose tissue in human obesity. *Mol Cell Endocrinol* **363**, 10-19

58. Segerstolpe, A., Palasantza, A., Eliasson, P., Andersson, E. M., Andreasson, A. C., Sun, X., Picelli, S., Sabirsh, A., Clausen, M., Bjursell, M. K., Smith, D. M., Kasper, M., Ammala, C., and Sandberg, R. (2016) Single-Cell Transcriptome Profiling of Human Pancreatic Islets in Health and Type 2 Diabetes. *Cell Metab* **24**, 593-607

59. Tang, S., Bao, H., Zhang, Y., Yao, J., Yang, P., and Chen, X. (2013) 14-3-3epsilon mediates the cell fate decision-making pathways in response of hepatocellular carcinoma to Bleomycin-induced DNA damage. *PLoS One* **8**, e55268

60. Bai, C., Tang, S., Bai, C., and Chen, X. (2014) Quantitative proteomic dissection of a native 14-3-3epsilon interacting protein complex associated with hepatocellular carcinoma. *Amino Acids* **46**, 841-852

61. Benzinger, A., Muster, N., Koch, H. B., Yates, J. R., 3rd, and Hermeking, H. (2005) Targeted proteomic analysis of 14-3-3 sigma, a p53 effector commonly silenced in cancer. *Mol Cell Proteomics* **4**, 785-795

Figure legends

Figure 1: Generation of TAP-14-3-3ζ mouse embryonic fibroblasts (MEFs) to elucidate the 14-3-3ζ interactome. (A) Schematic over-view of generation and use of TAP-14-3-3o MEFs to determine the 14-3-3ζ interactome during adipogenesis. **(B,C)** Verification of TAP-14-3-3ζ MEF adipogenesis by Oil Red-O incorporation, 7 days after induction (B), or *Pparg* mRNA expression by quantitative PCR (C), 2 days following induction (representative of n=4 independent experiments, *: $p<0.05$). **(D)** String-db (24) was used to visualize and cluster proteins according to their biological function, resulting in three distinct clusters: RNA splicing/processing factors, components of the ribosomal complex, and components of actin/tubulin network.

Figure 2: Induction of differentiation or depletion of 14-3-3ζ in 3T3-L1 cells promotes alternative splicing of mRNA. (A) Differential exon usage of genes involved in adipogenesis was compared in control or 14-3-3ζ-depleted 3T3-L1 cells undergoing adipocyte differentiation. Transcriptomic data was aligned via TopHat and subsequently subjected to DEXSeq analysis to measure differential exon usage. **(B)** To rule out an effect of 14-3-3ζ depletion on global RNA transcription, control (siCon) or 14-3-3ζ depleted cells (si14-3-3ζ) were incubated with 5-ethynyl uridine (EU), followed by Click-iT chemistry to detect newly synthesized RNA (scale bar= 10 μm; representative of n=4 experiments). **(C,D)** Comparison of genes exhibiting differential exon usage in control cells 0, 24, and 48 hours after differentiation (C) or control or 14-3-3ζ depleted cells at each time point (D). The overlapping regions of each Venn diagram denote genes that are common to each condition or treatment.

Figure 3: Known regulators of adipogenesis can be found within the 14-3-3ζ interactome (A) 3T3-L1 cells were transfected with a control siRNA (siCon) or siRNA against target mRNA, and knockdown efficiency was measured by quantitative PCR (n=4 per group, *: $p<0.05$). **(B, C)** Transient knockdown by siRNA of previously identified regulators of adipogenesis or those associated with the development of obesity was used to examine their contributions to adipocyte differentiation, as assessed by visualization of Oil Red-O incorporation (B), absorbance (490 nm, C) or *Pparg* mRNA expression (D) (n=4 per group, *:$p<0.05$ when compared to siCon-transfected differentiated cells).

Figure 4: RNA splicing proteins are required for 3T3-L1 adipogenesis

(A) 3T3-L1 cells were transfected with a control siRNA (siCon) or siRNA against target mRNA, and knockdown efficiency was measured by quantitative PCR (n=4 per group, *: p<0.05). **(B-D)** Transient knockdown by siRNA was used to examine the contributions of RNA splicing factors to adipocyte differentiation, as assessed by visualization of Oil Red-O incorporation (B), absorbance (490 nm, C) or *Pparg* mRNA expression (D) (n=4 per group, *:p<0.05 when compared to siCon-transfected differentiated cells). **(E)** 3T3-L1 cells were transfected with siRNAs against various targets, followed by induction of differentiation (+MDI) for 48 hours, and total RNA was isolated. Following RT-PCR for *Lpin1*, products were resolved on a 1% acrylamide gel (Inset: Schematic diagram of the RT-PCR-based approach to detect alternative spliced isoforms of *Lpin1*. Red bars denote primers used to detected the inclusion or exclusion of exon 7) (representative of n=4 independent experiments) **(F)** Densitometric analysis of *Lpin1* PCR products from panel E (*: p<0.05 when compared to undifferentiated (-MDI) 3T3-L1 cells).

Supplemental figure 1: *Pparg* exhibits differential exon usage during 3T3-L1 adipocyte differentiation. To confirm the ability of DEXSeq to detect genes exhibiting significant differential exon usage, transcriptomic data from undifferentiated and differentiating 3T3-L1 cells (48 hours post induction) were analyzed, and isoforms with differential use of exon 1 could be detected (n=4 per group).

Supplemental figure 2: Expression of candidate proteins from the 14-3-3ζ proteomic screen are largely unaffected by depletion of 14-3-3ζ. Transcriptomic data [GSE60745] (26) from 3T3-L1 cells transfected with control (siCon) or siRNA against 14-3-3ζ (si14-3-3ζ), followed by differentiation with an adipogenic cocktail (MDI) for up to 48 hours. The dataset was queried for expression profiles of 14-3-3ζ interacting partners that will be tested for their adipogenic contributions (Figure 3). (n=4 per group, *: p<0.05 when compared to t=0, $: p<0.05 when compared to siCon at respective time point).

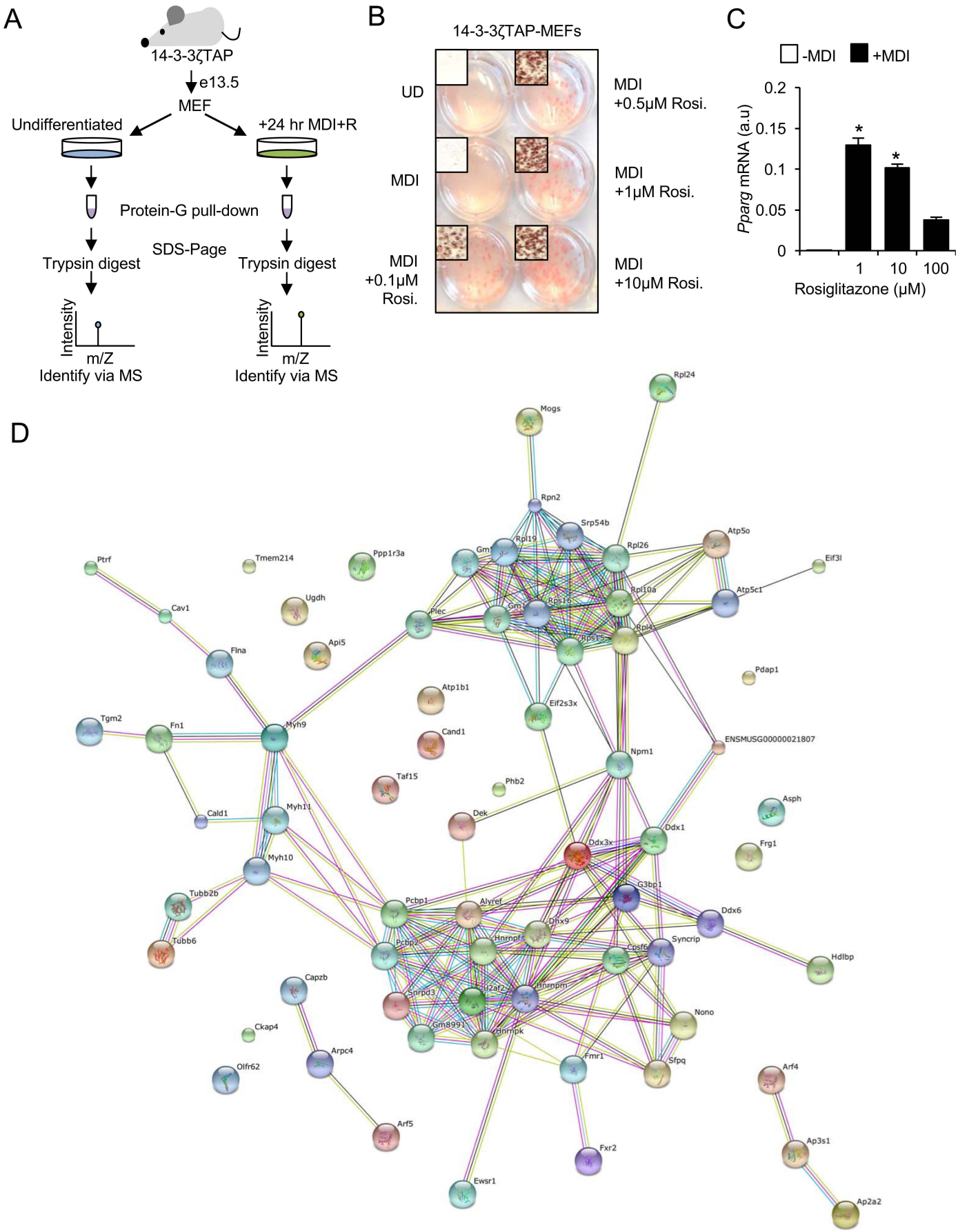
A
14-3-3ζTAP
e13.5
MEF
Undifferentiated
+24 hr MDI+R
Protein-G pull-down
SDS-Page
Trypsin digest
Trypsin digest
Intensity
m/Z
Identify via MS
Intensity
m/Z
Identify via MS
B
14-3-3ζTAP-MEFs
UD
MDI
MDI
+0.1μM
Rosi.
MDI
+0.5μM Rosi.
MDI
+1μM Rosi.
MDI
+10μM Rosi.
C
-MDI
+MDI
Pparg mRNA (a.u)
0.2
0.15
0.1
0.05
0
*
*
1
10
100
Rosiglitazone (μM)
D
Rpl24
Mogs
Rpn2
Srp54b
Rpl19
Gm
Rpl26
Atp5o
Eif3l
Ptrf
Tmem214
Ppp1r3a
Rpl10a
Atp5c1
Cav1
Ugdh
Plec
Gm
Rps16
Rpl4
Api5
Rps15
Flna
Pdap1
Atp1b1
Eif2s3x
Tgm2
Fn1
Myh9
Cand1
ENSMUSG00000021807
Npm1
Taf15
Phb2
Asph
Cald1
Myh11
Dek
Ddx1
Ddx3x
Frg1
Myh10
G3bp1
Tubb2b
Pcbp1
Alyref
Ddx6
Dhx9
Tubb6
Pcbp2
Hnrnpf
Cpsf6
Syncrip
Hdlbp
Capzb
Hnrnpm
Snrpd3
Nono
Ckap4
Gm8991
Hnrnpk
Arpc4
Fmr1
Sfpq
Olfr62
Arf4
Arf5
Fxr2
Ap3s1
Ewsr1
Ap2a2

A

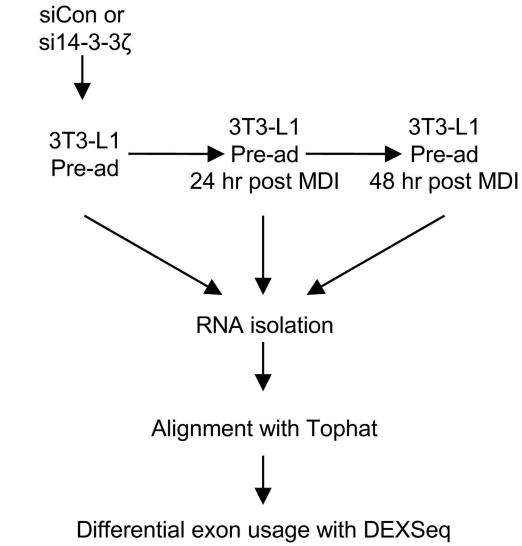

B

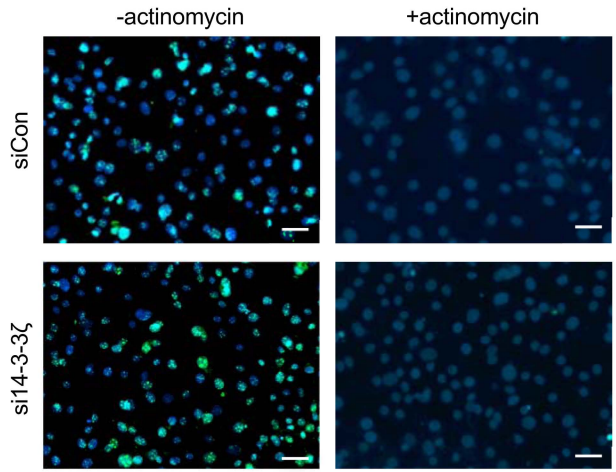

C

Comparison	hit p<0.05	locus unique p<0.05	gene unique
0 hr vs 24 hr	594	281	462
0 hr vs 48 hr	579	291	471

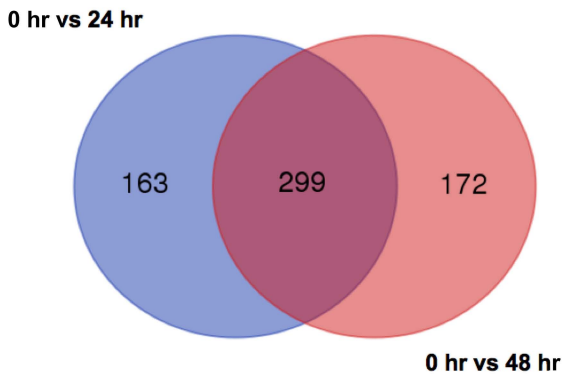

D

Comparison	hit p<0.05	locus unique p<0.05	gene unique
0 hr MDI siCon vs si14-3-3ζ	86	74	105
24 hr MDI siCon vs si14-3-3ζ	60	45	60
48 hr MDI siCon vs si14-3-3ζ	46	34	53

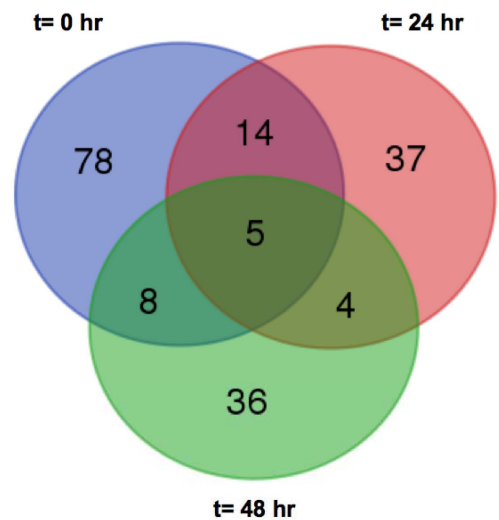

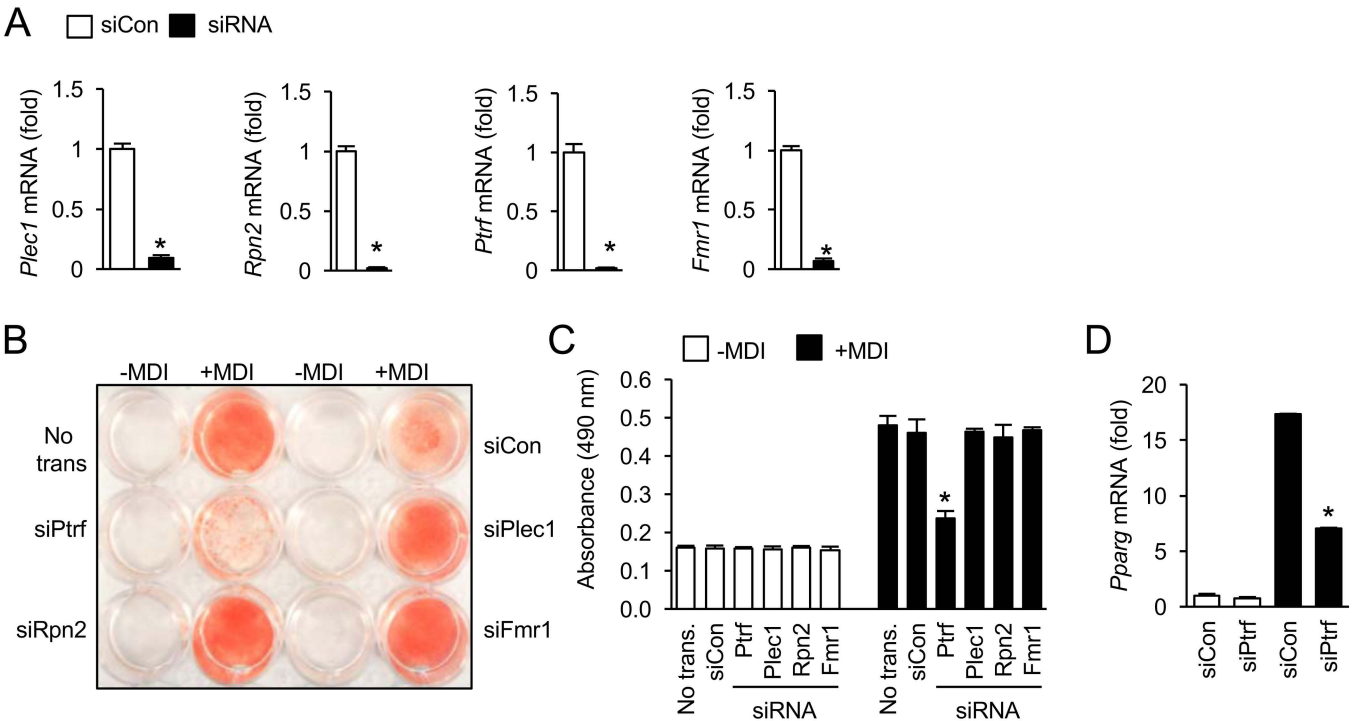
A
siCon
siRNA
Plec1 mRNA (fold)
Rpn2 mRNA (fold)
Ptrf mRNA (fold)
Fmr1 mRNA (fold)
1.5
1
0.5
0
*
B
-MDI
+MDI
-MDI
+MDI
No trans
siPtrf
siRpn2
siCon
siPlec1
siFmr1
C
-MDI
+MDI
Absorbance (490 nm)
0.6
0.5
0.4
0.3
0.2
0.1
0.0
No trans.
siCon
Ptrf
Plec1
Rpn2
Fmr1
siRNA
D
Pparg mRNA (fold)
20
15
10
5
0
siCon
siPtrf
siCon
siPtrf

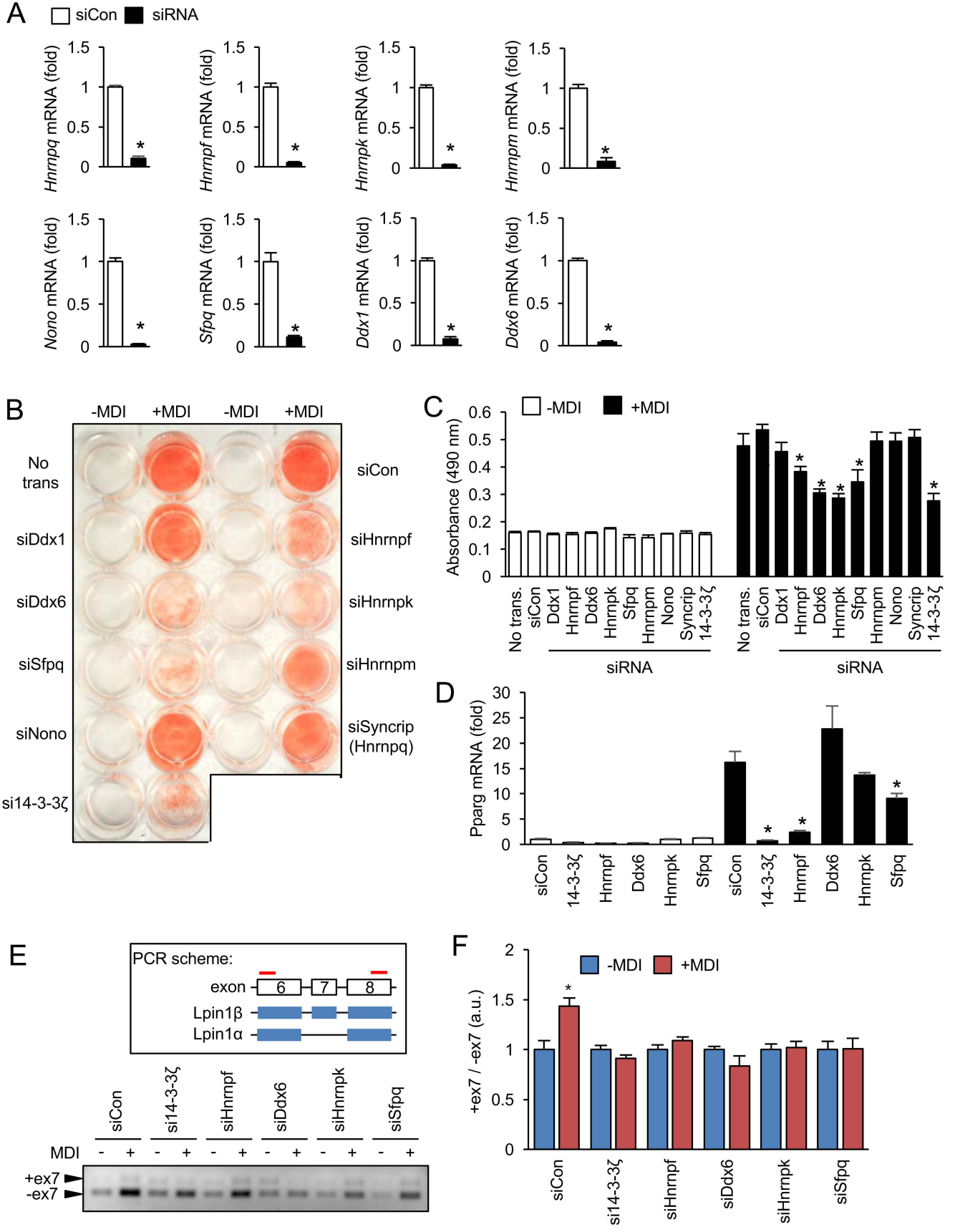
A
siCon
siRNA
Hnrnpq mRNA (fold)
Hnrnpf mRNA (fold)
Hnrnpk mRNA (fold)
Hnrnpm mRNA (fold)
Nono mRNA (fold)
Sfpq mRNA (fold)
Ddx1 mRNA (fold)
Ddx6 mRNA (fold)
1.5
1
0.5
0
*
B
-MDI
+MDI
-MDI
+MDI
No trans
siDdx1
siDdx6
siSfpq
siNono
si14-3-3ζ
siCon
siHnrnpf
siHnrnpk
siHnrnpm
siSyncrip (Hnrnpq)
C
-MDI
+MDI
Absorbance (490 nm)
0.6
0.5
0.4
0.3
0.2
0.1
0
No trans.
siCon
Ddx1
Hnrnpf
Ddx6
Hnrnpk
Sfpq
Hnrnpm
Nono
Syncrip
14-3-3ζ
siRNA
D
Pparg mRNA (fold)
30
25
20
15
10
5
0
siCon
14-3-3ζ
Hnrnpf
Ddx6
Hnrnpk
Sfpq
E
PCR scheme:
exon
6
7
8
Lpin1β
Lpin1α
siCon
si14-3-3ζ
siHnrnpf
siDdx6
siHnrnpk
siSfpq
MDI
-
+
+ex7
-ex7
F
-MDI
+MDI
+ex7 / -ex7 (a.u.)
2
1.5
1
0.5
0
siCon
si14-3-3ζ
siHnrnpf
siDdx6
siHnrnpk
siSfpq

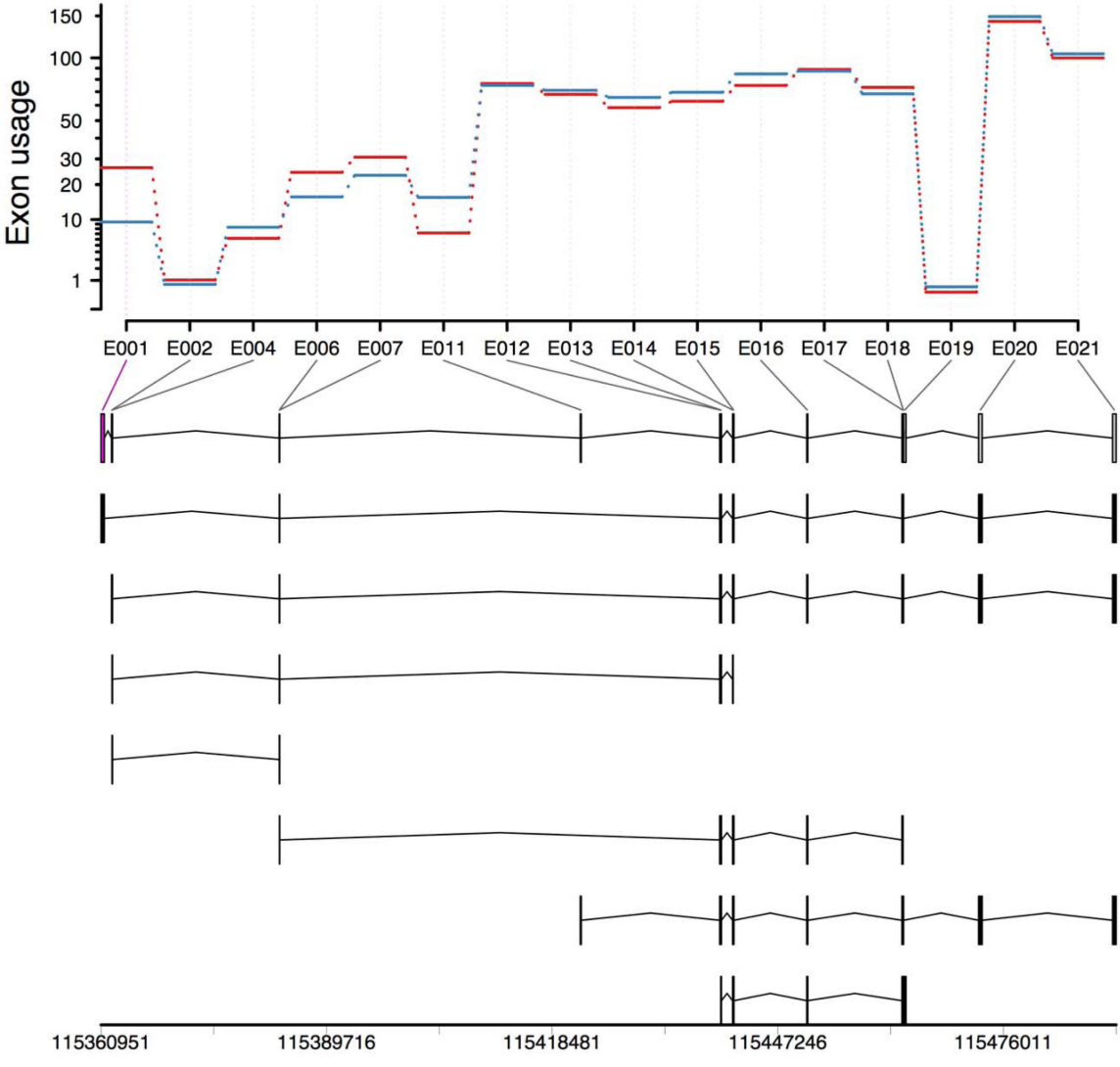
Exon usage
150
100
50
30
20
10
1
E001
E002
E004
E006
E007
E011
E012
E013
E014
E015
E016
E017
E018
E019
E020
E021
115360951
115389716
115418481
115447246
115476011

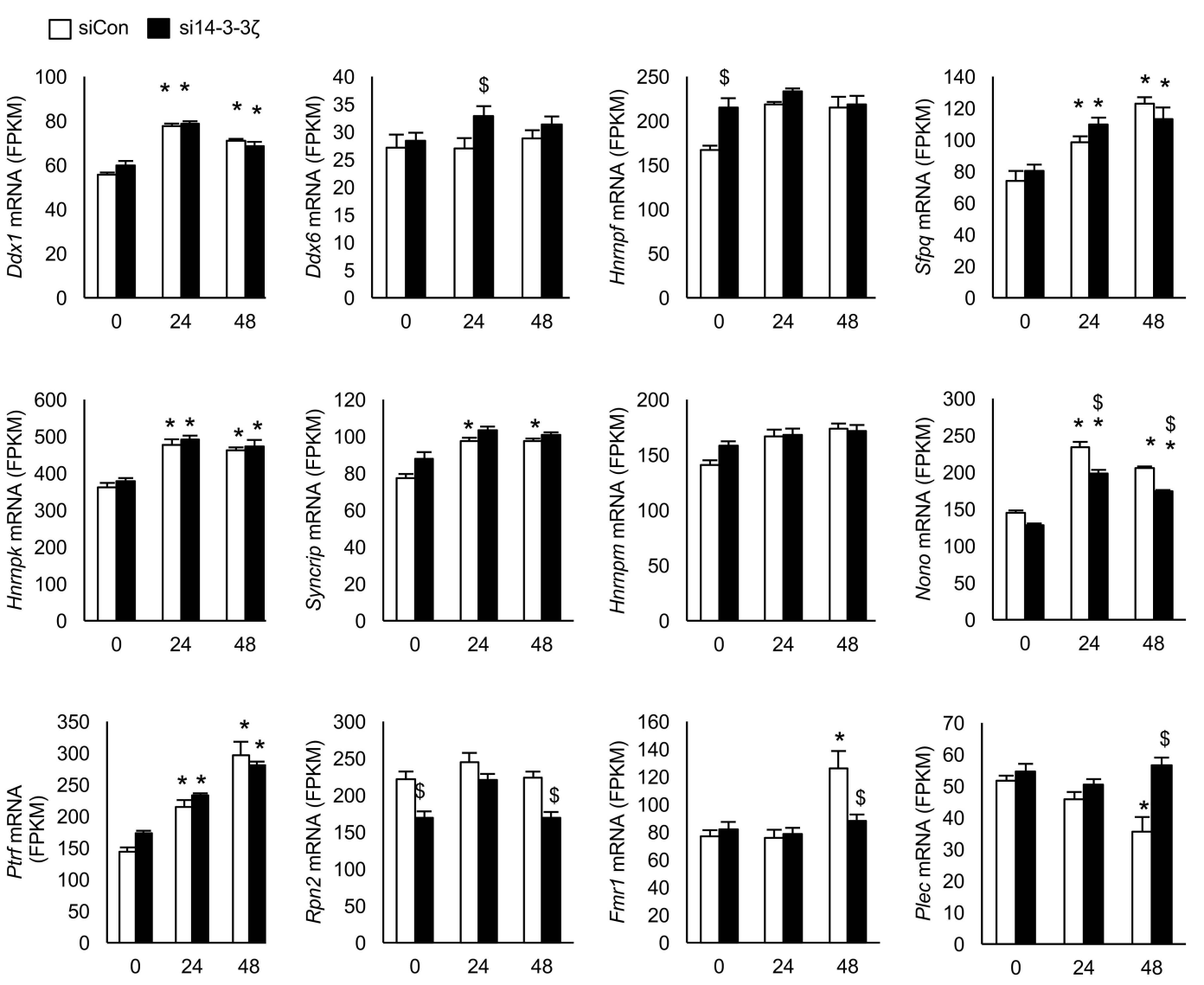
siCon
si14-3-3ζ
Ddx1 mRNA (FPKM)
Ddx6 mRNA (FPKM)
Hnrnpf mRNA (FPKM)
Sfpq mRNA (FPKM)
Hnrnpk mRNA (FPKM)
Syncrip mRNA (FPKM)
Hnrnpm mRNA (FPKM)
Nono mRNA (FPKM)
Ptrf mRNA (FPKM)
Rpn2 mRNA (FPKM)
Fmr1 mRNA (FPKM)
Plec mRNA (FPKM)
0
24
48

Table 1: Proteins with at least 2 unique peptides with a total spectral count in differentiated cell >=2 in comparison to undifferentiated cells

Accession	Description	Σ# Peptides	Total spectrum IP1	Total spectrum IP1	Total spectrum IP2	total spectrum IP2
Q8VDD5	Myosin-9 OS=Mus musculus GN=Myh9 PE=1 SV=4 - [MYH9_MOUSE]	102	278	129	7	2
Q4FK11	Non-POU-domain-containing, octamer binding protein OS=Mus musculus GN=Nono PE=2 SV=1 - [Q4FK11_MOUSE]	16	11	1	149	7
E9QMZ5	Uncharacterized protein OS=Mus musculus GN=Plec PE=4 SV=1 - [E9QMZ5_MOUSE]	123	101	41	74	23
E9QPE8	Uncharacterized protein OS=Mus musculus GN=Plec PE=4 SV=1 - [E9QPE8_MOUSE]	122	99	41	75	23
G5E8B8	Anastellin OS=Mus musculus GN=Fn1 PE=4 SV=1 - [G5E8B8_MOUSE]	46	60	21	58	11
Q61879	Myosin-10 OS=Mus musculus GN=Myh10 PE=1 SV=2 - [MYH10_MOUSE]	68	107	41	2	1
P97855	Ras GTPase-activating protein-binding protein 1 OS=Mus musculus GN=G3bp1 PE=1 SV=1 - [G3BP1_MOUSE]	20	20	6	94	45
P61979	Heterogeneous nuclear ribonucleoprotein K OS=Mus musculus GN=Hnrnpk PE=1 SV=1 - [HNRPK_MOUSE]	16	35	10	62	29
Q9R002	Interferon-activable protein 202 OS=Mus musculus GN=Ifi202 PE=1 SV=3 - [IFI2_MOUSE]	13	4	0	45	1
B7FAU9	Filamin, alpha OS=Mus musculus GN=Flna PE=4 SV=1 - [B7FAU9_MOUSE]	48	65	21	3	1
Q61033	Lamina-associated polypeptide 2, isoforms alpha/zeta OS=Mus musculus GN=Tmpo PE=1 SV=4 - [LAP2A_MOUSE]	19	13	3	31	1
B2RSN3	MCG1395 OS=Mus musculus GN=Tubb2b PE=2 SV=1 - [B2RSN3_MOUSE]	17	33	7	23	10
Q91VR5	ATP-dependent RNA helicase DDX1 OS=Mus musculus GN=Ddx1 PE=1 SV=1 - [DDX1_MOUSE]	29	16	3	42	17
P48962	ADP/ATP translocase 1 OS=Mus musculus GN=Slc25a4 PE=1 SV=4 - [ADT1_MOUSE]	14	27	6	29	13
P51881	ADP/ATP translocase 2 OS=Mus musculus GN=Slc25a5 PE=1 SV=3 - [ADT2_MOUSE]	12	25	6	27	10
Q60865	Caprin-1 OS=Mus musculus GN=Caprin1 PE=1 SV=2 - [CAPR1_MOUSE]	19	10	3	50	23
Q8BMK4	Cytoskeleton-associated protein 4 OS=Mus musculus GN=Ckap4 PE=2 SV=2 - [CKAP4_MOUSE]	17	22	5	22	6
B8JJG1	Novel protein (2810405J04Rik) OS=Mus musculus GN=Fam98a PE=4 SV=1 - [B8JJG1_MOUSE]	9	8	1	30	7
Q61029	Lamina-associated polypeptide 2, isoforms beta/delta/epsilon/gamma OS=Mus musculus GN=Tmpo PE=1 SV=4 - [LAP2B_MOUSE]	14	12	4	23	2
Q8VIJ6	Splicing factor, proline- and glutamine-rich OS=Mus musculus GN=Sfpq PE=1 SV=1 - [SFPQ_MOUSE]	19	7	2	39	16
P62702	40S ribosomal protein S4, X isoform OS=Mus musculus GN=Rps4x PE=2 SV=2 - [RS4X_MOUSE]	15	18	5	26	11
Q3TQX5	DEAD/H (Asp-Glu-Ala-Asp/His) box polypeptide 3, X-linked OS=Mus musculus GN=Ddx3x PE=2 SV=1 - [Q3TQX5_MOUSE]	19	14	2	26	11
Q4VA29	MCG140066 OS=Mus musculus GN=2700060E02Rik PE=2 SV=1 - [Q4VA29_MOUSE]	10	9	2	23	4
P14148	60S ribosomal protein L7 OS=Mus musculus GN=Rpl7 PE=2 SV=2 - [RL7_MOUSE]	13	19	0	6	0
Q3UMM1	Tubulin, beta 6 OS=Mus musculus GN=Tubb6 PE=2 SV=1 - [Q3UMM1_MOUSE]	13	18	2	11	2
G3UXT7	RNA-binding protein FUS (Fragment) OS=Mus musculus GN=Fus PE=4 SV=1 - [G3UXT7_MOUSE]	7	12	2	24	9
Q8VEM8	Phosphate carrier protein, mitochondrial OS=Mus musculus GN=Slc25a3 PE=1 SV=1 - [MPCP_MOUSE]	7	13	1	16	5
E9QPE7	Myosin-11 OS=Mus musculus GN=Myh11 PE=4 SV=1 - [E9QPE7_MOUSE]	18	34	13	2	0
A2A547	Ribosomal protein L19 OS=Mus musculus GN=Rpl19 PE=3 SV=1 - [A2A547_MOUSE]	6	11	1	13	1
P63038	60 kDa heat shock protein, mitochondrial OS=Mus musculus GN=Hspd1 PE=1 SV=1 - [CH60_MOUSE]	13	14	0	13	5
D3Z6C3	Protein Gm10119 OS=Mus musculus GN=Gm10119 PE=3 SV=1 - [D3Z6C3_MOUSE]	12	16	3	15	6
Q9DB20	ATP synthase subunit O, mitochondrial OS=Mus musculus GN=Atp5o PE=1 SV=1 - [ATPO_MOUSE]	11	22	7	14	7
O70475	UDP-glucose 6-dehydrogenase OS=Mus musculus GN=Ugdh PE=1 SV=1 - [UGDH_MOUSE]	14	17	0	5	1
A2APD4	Small nuclear ribonucleoprotein-associated protein OS=Mus musculus GN=Snrpb PE=3 SV=1 - [A2APD4_MOUSE]	5	5	2	19	1
O70309	Integrin beta-5 OS=Mus musculus GN=Itgb5 PE=2 SV=2 - [ITB5_MOUSE]	14	7	2	16	1
G3UZI2	Heterogeneous nuclear ribonucleoprotein Q OS=Mus musculus GN=Syncrip PE=4 SV=1 - [G3UZI2_MOUSE]	11	9	1	16	4
D3Z6U8	Fragile X mental retardation protein 1 homolog OS=Mus musculus GN=Fmr1 PE=4 SV=1 - [D3Z6U8_MOUSE]	15	8	3	21	7
O35841	Apoptosis inhibitor 5 OS=Mus musculus GN=Api5 PE=2 SV=2 - [API5_MOUSE]	11	8	1	12	1
A4FUS1	MCG123443 OS=Mus musculus GN=Rps16 PE=1 SV=1 - [A4FUS1_MOUSE]	12	9	4	24	11
Q3TLH4-5	Isoform 5 of Protein PRRC2C OS=Mus musculus GN=Prrc2c - [PRC2C_MOUSE]	11	5	1	14	1
P14869	60S acidic ribosomal protein P0 OS=Mus musculus GN=Rplp0 PE=1 SV=3 - [RLA0_MOUSE]	8	16	5	8	2
Q8QZY1	Eukaryotic translation initiation factor 3 subunit L OS=Mus musculus GN=Eif3l PE=1 SV=1 - [EIF3L_MOUSE]	5	7	0	8	0
P35922	Fragile X mental retardation protein 1 homolog OS=Mus musculus GN=Fmr1 PE=1 SV=1 - [FMR1_MOUSE]	15	7	3	21	10
Q03265	ATP synthase subunit alpha, mitochondrial OS=Mus musculus GN=Atp5a1 PE=1 SV=1 - [ATPA_MOUSE]	15	14	3	4	2
P63017	Heat shock cognate 71 kDa protein OS=Mus musculus GN=Hspa8 PE=1 SV=1 - [HSP7C_MOUSE]	13	9	2	12	6
P21981	Protein-glutamine gamma-glutamyltransferase 2 OS=Mus musculus GN=Tgm2 PE=1 SV=4 - [TGM2_MOUSE]	8	5	0	7	0
Q80UM7	Mannosyl-oligosaccharide glucosidase OS=Mus musculus GN=Mogs PE=2 SV=1 - [MOGS_MOUSE]	11	3	0	13	4
P26369	Splicing factor U2AF 65 kDa subunit OS=Mus musculus GN=U2af2 PE=1 SV=3 - [U2AF2_MOUSE]	7	7	0	8	3
A2AJM8	MCG7378 OS=Mus musculus GN=Sec61b PE=4 SV=1 - [A2AJM8_MOUSE]	3	3	1	9	0
P62242	40S ribosomal protein S8 OS=Mus musculus GN=Rps8 PE=1 SV=2 - [RS8_MOUSE]	7	12	3	3	1
P54823	Probable ATP-dependent RNA helicase DDX6 OS=Mus musculus GN=Ddx6 PE=2 SV=1 - [DDX6_MOUSE]	8	2	1	13	3
Q3TML6	Eukaryotic translation initiation factor 2, subunit 3, structural gene X-linked OS=Mus musculus GN=Eif2s3x PE=2 SV=1 - [Q3TML6_MOUSE]	6	7	1	8	3
P26041	Moesin OS=Mus musculus GN=Msn PE=1 SV=3 - [MOES_MOUSE]	13	5	0	12	6
P62983	Ubiquitin-40S ribosomal protein S27a OS=Mus musculus GN=Rps27a PE=1 SV=2 - [RS27A_MOUSE]	6	5	2	13	5
P52480	Pyruvate kinase isozymes M1/M2 OS=Mus musculus GN=Pkm2 PE=1 SV=4 - [KPYM_MOUSE]	4	2	0	8	0
Q5SUT0	Ewing sarcoma breakpoint region 1 OS=Mus musculus GN=Ewsr1 PE=2 SV=1 - [Q5SUT0_MOUSE]	5	6	1	6	1
E9Q7H5	Uncharacterized protein OS=Mus musculus GN=Gm8991 PE=4 SV=1 - [E9Q7H5_MOUSE]	6	3	0	10	3
Q8C2Q8	ATP synthase gamma chain OS=Mus musculus GN=Atp5c1 PE=2 SV=1 - [Q8C2Q8_MOUSE]	7	5	1	9	3
A2AMW0	Capping protein (Actin filament) muscle Z-line, beta OS=Mus musculus GN=Capzb PE=4 SV=1 - [A2AMW0_MOUSE]	7	13	6	3	0
P08121	Collagen alpha-1(III) chain OS=Mus musculus GN=Col3a1 PE=2 SV=4 - [CO3A1_MOUSE]	6	5	0	4	0
P11087-2	Isoform 2 of Collagen alpha-1(I) chain OS=Mus musculus GN=Col1a1 - [CO1A1_MOUSE]	10	3	1	8	1
Q9Z2X1-2	Isoform 2 of Heterogeneous nuclear ribonucleoprotein F OS=Mus musculus GN=Hnrnpf - [HNRPF_MOUSE]	3	4	1	7	1
P11499	Heat shock protein HSP 90-beta OS=Mus musculus GN=Hsp90ab1 PE=1 SV=3 - [HS90B_MOUSE]	11	6	1	6	2
P28301	Protein-lysine 6-oxidase OS=Mus musculus GN=Lox PE=2 SV=1 - [LYOX_MOUSE]	4	2	1	9	1
Q8VCQ8	Caldesmon 1 OS=Mus musculus GN=Cald1 PE=2 SV=1 - [Q8VCQ8_MOUSE]	13	12	6	4	1
P27659	60S ribosomal protein L3 OS=Mus musculus GN=Rpl3 PE=2 SV=3 - [RL3_MOUSE]	7	9	1	2	1
O35737	Heterogeneous nuclear ribonucleoprotein H OS=Mus musculus GN=Hnrnph1 PE=1 SV=3 - [HNRH1_MOUSE]	4	3	1	6	0
A2ACG7	Dolichyl-diphosphooligosaccharide--protein glycosyltransferase subunit 2 OS=Mus musculus GN=Rpn2 PE=4 SV=1 - [A2ACG7_MOUSE]	7	3	0	6	1
Q3TVI8	Pre-B-cell leukemia transcription factor-interacting protein 1 OS=Mus musculus GN=Pbxip1 PE=1 SV=2 - [PBIP1_MOUSE]	6	3	0	6	1
F6QCI0	Protein Taf15 (Fragment) OS=Mus musculus GN=Taf15 PE=4 SV=1 - [F6QCI0_MOUSE]	4	3	0	6	1
O88569-3	Isoform 3 of Heterogeneous nuclear ribonucleoproteins A2/B1 OS=Mus musculus GN=Hnrnpa2b1 - [ROA2_MOUSE]	5	4	1	6	1
O08583-2	Isoform 2 of THO complex subunit 4 OS=Mus musculus GN=Alyref - [THOC4_MOUSE]	3	2	0	8	2
O08573-2	Isoform Short of Galectin-9 OS=Mus musculus GN=Lgals9 - [LEG9_MOUSE]	2	2	1	7	0
Q564E8	Ribosomal protein L4 OS=Mus musculus GN=Rpl4 PE=2 SV=1 - [Q564E8_MOUSE]	8	7	3	6	2
B1ARA3	60S ribosomal protein L26 (Fragment) OS=Mus musculus GN=Rpl26 PE=4 SV=1 - [B1ARA3_MOUSE]	6	5	0	5	2
O35129	Prohibitin-2 OS=Mus musculus GN=Phb2 PE=1 SV=1 - [PHB2_MOUSE]	4	4	0	7	3
D3YTQ9	40S ribosomal protein S15 OS=Mus musculus GN=Rps15 PE=3 SV=1 - [D3YTQ9_MOUSE]	3	6	1	2	0
Q6ZWX6	Eukaryotic translation initiation factor 2 subunit 1 OS=Mus musculus GN=Eif2s1 PE=1 SV=3 - [IF2A_MOUSE]	5	4	1	4	0
D3Z3R1	60S ribosomal protein L36 OS=Mus musculus GN=Gm5745 PE=3 SV=1 - [D3Z3R1_MOUSE]	5	3	1	6	1
P17427	AP-2 complex subunit alpha-2 OS=Mus musculus GN=Ap2a2 PE=1 SV=2 - [AP2A2_MOUSE]	8	3	1	7	2
P56480	ATP synthase subunit beta, mitochondrial OS=Mus musculus GN=Atp5b PE=1 SV=2 - [ATPB_MOUSE]	9	2	1	8	2
Q8CBM2	Aspartate-beta-hydroxylase OS=Mus musculus GN=Asph PE=2 SV=1 - [Q8CBM2_MOUSE]	8	4	0	6	3
Q6NVF9	Cleavage and polyadenylation specificity factor subunit 6 OS=Mus musculus GN=Cpsf6 PE=1 SV=1 - [CPSF6_MOUSE]	6	4	0	6	3
Q5SQB0	Nucleophosmin OS=Mus musculus GN=Npm1 PE=2 SV=1 - [Q5SQB0_MOUSE]	5	6	0	2	1
Q6A0A9	Constitutive coactivator of PPAR-gamma-like protein 1 OS=Mus musculus GN=FAM120A PE=1 SV=2 - [F120A_MOUSE]	5	2	0	4	0
P14576	Signal recognition particle 54 kDa protein OS=Mus musculus GN=Srp54 PE=1 SV=2 - [SRP54_MOUSE]	4	2	0	4	0
P63087	Serine/threonine-protein phosphatase PP1-gamma catalytic subunit OS=Mus musculus GN=Ppp1cc PE=1 SV=1 - [PP1G_MOUSE]	4	4	0	2	0
P80315	T-complex protein 1 subunit delta OS=Mus musculus GN=Cct4 PE=1 SV=3 - [TCPD_MOUSE]	4	3	0	3	0
P62960	Nuclease-sensitive element-binding protein 1 OS=Mus musculus GN=Ybx1 PE=1 SV=3 - [YBOX1_MOUSE]	3	2	0	5	1
P97376	Protein FRG1 OS=Mus musculus GN=Frg1 PE=1 SV=2 - [FRG1_MOUSE]	3	2	0	5	1
Q3U4Z7	High density lipoprotein (HDL) binding protein, isoform CRA_d OS=Mus musculus GN=Hdlbp PE=2 SV=1 - [Q3U4Z7_MOUSE]	7	3	0	4	1
B2RTB0	MCG17262 OS=Mus musculus GN=Pdap1 PE=2 SV=1 - [B2RTB0_MOUSE]	4	3	0	4	1
P60335	Poly(rC)-binding protein 1 OS=Mus musculus GN=Pcbp1 PE=1 SV=1 - [PCBP1_MOUSE]	4	3	0	4	1
P47911	60S ribosomal protein L6 OS=Mus musculus GN=Rpl6 PE=1 SV=3 - [RL6_MOUSE]	6	8	4	2	0
Q61990-2	Isoform 2 of Poly(rC)-binding protein 2 OS=Mus musculus GN=Pcbp2 - [PCBP2_MOUSE]	4	2	1	6	1
P62267	40S ribosomal protein S23 OS=Mus musculus GN=Rps23 PE=2 SV=3 - [RS23_MOUSE]	5	4	1	6	3
D3Z148	Caveolin (Fragment) OS=Mus musculus GN=Cav1 PE=3 SV=2 - [D3Z148_MOUSE]	4	2	0	3	0
P84084	ADP-ribosylation factor 5 OS=Mus musculus GN=Arf5 PE=2 SV=2 - [ARF5_MOUSE]	4	2	0	3	0
O54724	Polymerase I and transcript release factor OS=Mus musculus GN=Ptrf PE=1 SV=1 - [PTRF_MOUSE]	3	2	0	3	0
E9Q132	60S ribosomal protein L24 OS=Mus musculus GN=Rpl24 PE=4 SV=1 - [E9Q132_MOUSE]	3	4	1	2	0

Table 2: Identification of novel interactors with 14-3-3 proteins

****Compared to data from Johnson et al. Mol Cell Proteomics (2011) M110 005751**

Accession	Description	Previously reported to interact with 14-3-3ζ
Q8VDD5	Myosin-9 OS=Mus musculus GN=Myh9 PE=1 SV=4 - [MYH9_MOUSE]	Yes
Q4FK11	Non-POU-domain-containing, octamer binding protein OS=Mus musculus GN=Nono PE=2 SV=1 - [Q4FK11_MOUSE]	No
E9QMZ5	Uncharacterized protein OS=Mus musculus GN=Plec PE=4 SV=1 - [E9QMZ5_MOUSE]	No
E9QPE8	Uncharacterized protein OS=Mus musculus GN=Plec PE=4 SV=1 - [E9QPE8_MOUSE]	No
G5E8B8	Anastellin OS=Mus musculus GN=Fn1 PE=4 SV=1 - [G5E8B8_MOUSE]	No
Q61879	Myosin-10 OS=Mus musculus GN=Myh10 PE=1 SV=2 - [MYH10_MOUSE]	Yes
P97855	Ras GTPase-activating protein-binding protein 1 OS=Mus musculus GN=G3bp1 PE=1 SV=1 - [G3BP1_MOUSE]	Yes
P61979	Heterogeneous nuclear ribonucleoprotein K OS=Mus musculus GN=Hnrnpk PE=1 SV=1 - [HNRPK_MOUSE]	Yes
Q9R002	Interferon-activable protein 202 OS=Mus musculus GN=Ifi202 PE=1 SV=3 - [IFI2_MOUSE]	No
B7FAU9	Filamin, alpha OS=Mus musculus GN=Flna PE=4 SV=1 - [B7FAU9_MOUSE]	No
Q61033	Lamina-associated polypeptide 2, isoforms alpha/zeta OS=Mus musculus GN=Tmpo PE=1 SV=4 - [LAP2A_MOUSE]	Yes
B2RSN3	MCG1395 OS=Mus musculus GN=Tubb2b PE=2 SV=1 - [B2RSN3_MOUSE]	Yes
Q91VR5	ATP-dependent RNA helicase DDX1 OS=Mus musculus GN=Ddx1 PE=1 SV=1 - [DDX1_MOUSE]	Yes
P48962	ADP/ATP translocase 1 OS=Mus musculus GN=Slc25a4 PE=1 SV=4 - [ADT1_MOUSE]	Yes
P51881	ADP/ATP translocase 2 OS=Mus musculus GN=Slc25a5 PE=1 SV=3 - [ADT2_MOUSE]	Yes
Q60865	Caprin-1 OS=Mus musculus GN=Caprin1 PE=1 SV=2 - [CAPR1_MOUSE]	Yes
Q8BMK4	Cytoskeleton-associated protein 4 OS=Mus musculus GN=Ckap4 PE=2 SV=2 - [CKAP4_MOUSE]	Yes
B8JJG1	Novel protein (2810405J04Rik) OS=Mus musculus GN=Fam98a PE=4 SV=1 - [B8JJG1_MOUSE]	No
Q61029	Lamina-associated polypeptide 2, isoforms beta/delta/epsilon/gamma OS=Mus musculus GN=Tmpo PE=1 SV=4 - [LAP2B_MOUSE]	Yes
Q8VIJ6	Splicing factor, proline- and glutamine-rich OS=Mus musculus GN=Sfpq PE=1 SV=1 - [SFPQ_MOUSE]	Yes
P62702	40S ribosomal protein S4, X isoform OS=Mus musculus GN=Rps4x PE=2 SV=2 - [RS4X_MOUSE]	Yes
Q3TQX5	DEAD/H (Asp-Glu-Ala-Asp/His) box polypeptide 3, X-linked OS=Mus musculus GN=Ddx3x PE=2 SV=1 - [Q3TQX5_MOUSE]	No
Q4VA29	MCG140066 OS=Mus musculus GN=2700060E02Rik PE=2 SV=1 - [Q4VA29_MOUSE]	No
P14148	60S ribosomal protein L7 OS=Mus musculus GN=Rpl7 PE=2 SV=2 - [RL7_MOUSE]	Yes
Q3UMM1	Tubulin, beta 6 OS=Mus musculus GN=Tubb6 PE=2 SV=1 - [Q3UMM1_MOUSE]	No
G3UXT7	RNA-binding protein FUS (Fragment) OS=Mus musculus GN=Fus PE=4 SV=1 - [G3UXT7_MOUSE]	No
Q8VEM8	Phosphate carrier protein, mitochondrial OS=Mus musculus GN=Slc25a3 PE=1 SV=1 - [MPCP_MOUSE]	Yes
E9QPE7	Myosin-11 OS=Mus musculus GN=Myh11 PE=4 SV=1 - [E9QPE7_MOUSE]	No
A2A547	Ribosomal protein L19 OS=Mus musculus GN=Rpl19 PE=3 SV=1 - [A2A547_MOUSE]	No
P63038	60 kDa heat shock protein, mitochondrial OS=Mus musculus GN=Hspd1 PE=1 SV=1 - [CH60_MOUSE]	Yes
D3Z6C3	Protein Gm10119 OS=Mus musculus GN=Gm10119 PE=3 SV=1 - [D3Z6C3_MOUSE]	No
Q9DB20	ATP synthase subunit O, mitochondrial OS=Mus musculus GN=Atp5o PE=1 SV=1 - [ATPO_MOUSE]	Yes
O70475	UDP-glucose 6-dehydrogenase OS=Mus musculus GN=Ugdh PE=1 SV=1 - [UGDH_MOUSE]	No
A2APD4	Small nuclear ribonucleoprotein-associated protein OS=Mus musculus GN=Snrpb PE=3 SV=1 - [A2APD4_MOUSE]	No
O70309	Integrin beta-5 OS=Mus musculus GN=Itgb5 PE=2 SV=2 - [ITB5_MOUSE]	No
G3UZI2	Heterogeneous nuclear ribonucleoprotein Q OS=Mus musculus GN=Syncrip PE=4 SV=1 - [G3UZI2_MOUSE]	No
D3Z6U8	Fragile X mental retardation protein 1 homolog OS=Mus musculus GN=Fmr1 PE=4 SV=1 - [D3Z6U8_MOUSE]	No
O35841	Apoptosis inhibitor 5 OS=Mus musculus GN=Api5 PE=2 SV=2 - [API5_MOUSE]	No
A4FUS1	MCG123443 OS=Mus musculus GN=Rps16 PE=1 SV=1 - [A4FUS1_MOUSE]	No
Q3TLH4-5	Isoform 5 of Protein PRRC2C OS=Mus musculus GN=Prrc2c - [PRC2C_MOUSE]	No
P14869	60S acidic ribosomal protein P0 OS=Mus musculus GN=Rplp0 PE=1 SV=3 - [RLA0_MOUSE]	Yes
Q8QZY1	Eukaryotic translation initiation factor 3 subunit L OS=Mus musculus GN=Eif3l PE=1 SV=1 - [EIF3L_MOUSE]	No
P35922	Fragile X mental retardation protein 1 homolog OS=Mus musculus GN=Fmr1 PE=1 SV=1 - [FMR1_MOUSE]	Yes
Q03265	ATP synthase subunit alpha, mitochondrial OS=Mus musculus GN=Atp5a1 PE=1 SV=1 - [ATPA_MOUSE]	Yes
P63017	Heat shock cognate 71 kDa protein OS=Mus musculus GN=Hspa8 PE=1 SV=1 - [HSP7C_MOUSE]	Yes
P21981	Protein-glutamine gamma-glutamyltransferase 2 OS=Mus musculus GN=Tgm2 PE=1 SV=4 - [TGM2_MOUSE]	Yes
Q80UM7	Mannosyl-oligosaccharide glucosidase OS=Mus musculus GN=Mogs PE=2 SV=1 - [MOGS_MOUSE]	Yes
P26369	Splicing factor U2AF 65 kDa subunit OS=Mus musculus GN=U2af2 PE=1 SV=3 - [U2AF2_MOUSE]	No
A2AJM8	MCG7378 OS=Mus musculus GN=Sec61b PE=4 SV=1 - [A2AJM8_MOUSE]	No
P62242	40S ribosomal protein S8 OS=Mus musculus GN=Rps8 PE=1 SV=2 - [RS8_MOUSE]	Yes
P54823	Probable ATP-dependent RNA helicase DDX6 OS=Mus musculus GN=Ddx6 PE=2 SV=1 - [DDX6_MOUSE]	Yes
Q3TML6	Eukaryotic translation initiation factor 2, subunit 3, structural gene X-linked OS=Mus musculus GN=Eif2s3x PE=2 SV=1 - [Q3TML6_MOUSE]	No
P26041	Moesin OS=Mus musculus GN=Msn PE=1 SV=3 - [MOES_MOUSE]	Yes
P62983	Ubiquitin-40S ribosomal protein S27a OS=Mus musculus GN=Rps27a PE=1 SV=2 - [RS27A_MOUSE]	Yes
P52480	Pyruvate kinase isozymes M1/M2 OS=Mus musculus GN=Pkm2 PE=1 SV=4 - [KPYM_MOUSE]	Yes
Q5SUT0	Ewing sarcoma breakpoint region 1 OS=Mus musculus GN=Ewsr1 PE=2 SV=1 - [Q5SUT0_MOUSE]	No
E9Q7H5	Uncharacterized protein OS=Mus musculus GN=Gm8991 PE=4 SV=1 - [E9Q7H5_MOUSE]	No
Q8C2Q8	ATP synthase gamma chain OS=Mus musculus GN=Atp5c1 PE=2 SV=1 - [Q8C2Q8_MOUSE]	No
A2AMW0	Capping protein (Actin filament) muscle Z-line, beta OS=Mus musculus GN=Capzb PE=4 SV=1 - [A2AMW0_MOUSE]	No
P08121	Collagen alpha-1(III) chain OS=Mus musculus GN=Col3a1 PE=2 SV=4 - [CO3A1_MOUSE]	Yes
P11087-2	Isoform 2 of Collagen alpha-1(I) chain OS=Mus musculus GN=Col1a1 - [CO1A1_MOUSE]	Yes
Q9Z2X1-2	Isoform 2 of Heterogeneous nuclear ribonucleoprotein F OS=Mus musculus GN=Hnrnpf - [HNRPF_MOUSE]	Yes
P11499	Heat shock protein HSP 90-beta OS=Mus musculus GN=Hsp90ab1 PE=1 SV=3 - [HS90B_MOUSE]	Yes
P28301	Protein-lysine 6-oxidase OS=Mus musculus GN=Lox PE=2 SV=1 - [LYOX_MOUSE]	Yes
Q8VCQ8	Caldesmon 1 OS=Mus musculus GN=Cald1 PE=2 SV=1 - [Q8VCQ8_MOUSE]	No
P27659	60S ribosomal protein L3 OS=Mus musculus GN=Rpl3 PE=2 SV=3 - [RL3_MOUSE]	Yes
O35737	Heterogeneous nuclear ribonucleoprotein H OS=Mus musculus GN=Hnrnph1 PE=1 SV=3 - [HNRH1_MOUSE]	Yes
A2ACG7	Dolichyl-diphosphooligosaccharide--protein glycosyltransferase subunit 2 OS=Mus musculus GN=Rpn2 PE=4 SV=1 - [A2ACG7_MOUSE]	No
Q3TVI8	Pre-B-cell leukemia transcription factor-interacting protein 1 OS=Mus musculus GN=Pbxip1 PE=1 SV=2 - [PBIP1_MOUSE]	No
F6QCI0	Protein Taf15 (Fragment) OS=Mus musculus GN=Taf15 PE=4 SV=1 - [F6QCI0_MOUSE]	No
O88569-3	Isoform 3 of Heterogeneous nuclear ribonucleoproteins A2/B1 OS=Mus musculus GN=Hnrnpa2b1 - [ROA2_MOUSE]	Yes
O08583-2	Isoform 2 of THO complex subunit 4 OS=Mus musculus GN=Alyref - [THOC4_MOUSE]	Yes
O08573-2	Isoform Short of Galectin-9 OS=Mus musculus GN=Lgals9 - [LEG9_MOUSE]	Yes
Q564E8	Ribosomal protein L4 OS=Mus musculus GN=Rpl4 PE=2 SV=1 - [Q564E8_MOUSE]	No
B1ARA3	60S ribosomal protein L26 (Fragment) OS=Mus musculus GN=Rpl26 PE=4 SV=1 - [B1ARA3_MOUSE]	No
O35129	Prohibitin-2 OS=Mus musculus GN=Phb2 PE=1 SV=1 - [PHB2_MOUSE]	Yes
D3YTQ9	40S ribosomal protein S15 OS=Mus musculus GN=Rps15 PE=3 SV=1 - [D3YTQ9_MOUSE]	No
Q6ZWX6	Eukaryotic translation initiation factor 2 subunit 1 OS=Mus musculus GN=Eif2s1 PE=1 SV=3 - [IF2A_MOUSE]	Yes
D3Z3R1	60S ribosomal protein L36 OS=Mus musculus GN=Gm5745 PE=3 SV=1 - [D3Z3R1_MOUSE]	No
P17427	AP-2 complex subunit alpha-2 OS=Mus musculus GN=Ap2a2 PE=1 SV=2 - [AP2A2_MOUSE]	No
P56480	ATP synthase subunit beta, mitochondrial OS=Mus musculus GN=Atp5b PE=1 SV=2 - [ATPB_MOUSE]	Yes
Q8CBM2	Aspartate-beta-hydroxylase OS=Mus musculus GN=Asph PE=2 SV=1 - [Q8CBM2_MOUSE]	No
Q6NVF9	Cleavage and polyadenylation specificity factor subunit 6 OS=Mus musculus GN=Cpsf6 PE=1 SV=1 - [CPSF6_MOUSE]	Yes
Q5SQB0	Nucleophosmin OS=Mus musculus GN=Npm1 PE=2 SV=1 - [Q5SQB0_MOUSE]	No
Q6A0A9	Constitutive coactivator of PPAR-gamma-like protein 1 OS=Mus musculus GN=FAM120A PE=1 SV=2 - [F120A_MOUSE]	Yes
P14576	Signal recognition particle 54 kDa protein OS=Mus musculus GN=Srp54 PE=1 SV=2 - [SRP54_MOUSE]	No
P63087	Serine/threonine-protein phosphatase PP1-gamma catalytic subunit OS=Mus musculus GN=Ppp1cc PE=1 SV=1 - [PP1G_MOUSE]	Yes
P80315	T-complex protein 1 subunit delta OS=Mus musculus GN=Cct4 PE=1 SV=3 - [TCPD_MOUSE]	Yes
P62960	Nuclease-sensitive element-binding protein 1 OS=Mus musculus GN=Ybx1 PE=1 SV=3 - [YBOX1_MOUSE]	Yes
P97376	Protein FRG1 OS=Mus musculus GN=Frg1 PE=1 SV=2 - [FRG1_MOUSE]	No
Q3U4Z7	High density lipoprotein (HDL) binding protein, isoform CRA_d OS=Mus musculus GN=Hdlbp PE=2 SV=1 - [Q3U4Z7_MOUSE]	No
B2RTB0	MCG17262 OS=Mus musculus GN=Pdap1 PE=2 SV=1 - [B2RTB0_MOUSE]	No
P60335	Poly(rC)-binding protein 1 OS=Mus musculus GN=Pcbp1 PE=1 SV=1 - [PCBP1_MOUSE]	Yes
P47911	60S ribosomal protein L6 OS=Mus musculus GN=Rpl6 PE=1 SV=3 - [RL6_MOUSE]	Yes
Q61990-2	Isoform 2 of Poly(rC)-binding protein 2 OS=Mus musculus GN=Pcbp2 - [PCBP2_MOUSE]	Yes
P62267	40S ribosomal protein S23 OS=Mus musculus GN=Rps23 PE=2 SV=3 - [RS23_MOUSE]	Yes
D3Z148	Caveolin (Fragment) OS=Mus musculus GN=Cav1 PE=3 SV=2 - [D3Z148_MOUSE]	No
P84084	ADP-ribosylation factor 5 OS=Mus musculus GN=Arf5 PE=2 SV=2 - [ARF5_MOUSE]	Yes
O54724	Polymerase I and transcript release factor OS=Mus musculus GN=Ptrf PE=1 SV=1 - [PTRF_MOUSE]	Yes
E9Q132	60S ribosomal protein L24 OS=Mus musculus GN=Rpl24 PE=4 SV=1 - [E9Q132_MOUSE]	No
O54890	Integrin beta-3 OS=Mus musculus GN=Itgb3 PE=2 SV=2 - [ITB3_MOUSE]	No
O88477	Insulin-like growth factor 2 mRNA-binding protein 1 OS=Mus musculus GN=Igf2bp1 PE=1 SV=1 - [IF2B1_MOUSE]	Yes
P61750	ADP-ribosylation factor 4 OS=Mus musculus GN=Arf4 PE=2 SV=2 - [ARF4_MOUSE]	Yes
Q9CR67	Transmembrane protein 33 OS=Mus musculus GN=Tmem33 PE=2 SV=1 - [TMM33_MOUSE]	Yes
Q5XJF6	Ribosomal protein OS=Mus musculus GN=Rpl10a PE=2 SV=1 - [Q5XJF6_MOUSE]	No
Q3THB3	Heterogeneous nuclear ribonucleoprotein M OS=Mus musculus GN=Hnrnpm PE=2 SV=1 - [Q3THB3_MOUSE]	No
Q6P5B5	Fragile X mental retardation syndrome-related protein 2 OS=Mus musculus GN=Fxr2 PE=2 SV=1 - [Q6P5B5_MOUSE]	No
D3Z6S1	Uncharacterized protein OS=Mus musculus GN=Tmem214 PE=4 SV=1 - [D3Z6S1_MOUSE]	No
P11152	Lipoprotein lipase OS=Mus musculus GN=Lpl PE=1 SV=3 - [LIPL_MOUSE]	Yes
Q9DCR2	AP-3 complex subunit sigma-1 OS=Mus musculus GN=Ap3s1 PE=1 SV=2 - [AP3S1_MOUSE]	No
P59999	Actin-related protein 2/3 complex subunit 4 OS=Mus musculus GN=Arpc4 PE=1 SV=3 - [ARPC4_MOUSE]	Yes
P49312	Heterogeneous nuclear ribonucleoprotein A1 OS=Mus musculus GN=Hnrnpa1 PE=1 SV=2 - [ROA1_MOUSE]	Yes
P61358	60S ribosomal protein L27 OS=Mus musculus GN=Rpl27 PE=2 SV=2 - [RL27_MOUSE]	Yes
O54734	Dolichyl-diphosphooligosaccharide--protein glycosyltransferase 48 kDa subunit OS=Mus musculus GN=Ddost PE=1 SV=2 - [OST48_MOUSE]	Yes
Q07235	Glia-derived nexin OS=Mus musculus GN=Serpine2 PE=2 SV=2 - [GDN_MOUSE]	No
Q7TNV0	Protein DEK OS=Mus musculus GN=Dek PE=1 SV=1 - [DEK_MOUSE]	Yes
Q922B2	Aspartate--tRNA ligase, cytoplasmic OS=Mus musculus GN=Dars PE=2 SV=2 - [SYDC_MOUSE]	No
P62320	Small nuclear ribonucleoprotein Sm D3 OS=Mus musculus GN=Snrpd3 PE=1 SV=1 - [SMD3_MOUSE]	Yes
P15864	Histone H1.2 OS=Mus musculus GN=Hist1h1c PE=1 SV=2 - [H12_MOUSE]	Yes
Q8R0W0	Epiplakin OS=Mus musculus GN=Eppk1 PE=1 SV=2 - [EPIPL_MOUSE]	No
Q6ZQ38	Cullin-associated NEDD8-dissociated protein 1 OS=Mus musculus GN=Cand1 PE=2 SV=2 - [CAND1_MOUSE]	Yes

Total # of novel interactors: 56

Table 3: Gene ontology classification of proteomic hits by biological process

Annotation Cluster 1		Enrichment Score: 10.542304553852539		
Term		**p-value**	**Benjamini**	**FDR**
GO:0006397	mRNA processing	2.80E-12	1.18E-09	4.33E-09
GO:0008380	RNA splicing	8.22E-12	2.31E-09	1.27E-08
GO:0016071	mRNA metabolic process	2.70E-11	5.71E-09	4.18E-08
GO:0006396	RNA processing	1.09E-09	1.84E-07	1.68E-06

Annotation Cluster 2		Enrichment Score: 2.9768010746589035		
Term		**p-value**	**Benjamini**	**FDR**
GO:0065003	macromolecular complex assembly	1.23E-04	0.01719154	0.19018503
GO:0006461	protein complex assembly	1.87E-04	0.01956598	0.28880909
GO:0070271	protein complex biogenesis	1.87E-04	0.01956598	0.28880909
GO:0043933	macromolecular complex subunit organization	2.40E-04	0.02229116	0.37052613
GO:0034621	cellular macromolecular complex subunit organization	0.001634086	0.10877737	2.49672826
GO:0034622	cellular macromolecular complex assembly	0.004135111	0.20818502	6.20540124
GO:0043623	cellular protein complex assembly	0.00690653	0.26524962	10.1607298
GO:0051258	protein polymerization	0.031762743	0.57358582	39.2881889

Annotation Cluster 3		Enrichment Score: 2.7758570598049186		
Term		**p-value**	**Benjamini**	**FDR**
GO:0015931	nucleobase, nucleoside, nucleotide and nucleic acid transport	1.65E-04	0.01976438	0.25533903
GO:0051236	establishment of RNA localization	0.001160158	0.09343294	1.77868077
GO:0050658	RNA transport	0.001160158	0.09343294	1.77868077
GO:0050657	nucleic acid transport	0.001160158	0.09343294	1.77868077
GO:0006403	RNA localization	0.001227278	0.09002225	1.88067318

Annotation Cluster 4		Enrichment Score: 1.3081305561358054		
Term		**p-value**	**Benjamini**	**FDR**
GO:0015986	ATP synthesis coupled proton transport	0.002165467	0.13143078	3.29598278
GO:0015985	energy coupled proton transport, down electrochemical gradient	0.002165467	0.13143078	3.29598278
GO:0034220	ion transmembrane transport	0.00311983	0.17188096	4.71608221
GO:0015992	proton transport	0.005711473	0.26103289	8.47469156
GO:0006818	hydrogen transport	0.006023853	0.24696352	8.91824507
GO:0006119	oxidative phosphorylation	0.007021577	0.25748192	10.3215008
GO:0006754	ATP biosynthetic process	0.019701699	0.53433002	26.4817286
GO:0046034	ATP metabolic process	0.025117659	0.59165663	32.5166079
GO:0009201	ribonucleoside triphosphate biosynthetic process	0.027334987	0.59373718	34.8509636
GO:0009206	purine ribonucleoside triphosphate biosynthetic process	0.027334987	0.59373718	34.8509636
GO:0009145	purine nucleoside triphosphate biosynthetic process	0.028096637	0.59012787	35.6352295
GO:0009142	nucleoside triphosphate biosynthetic process	0.02886954	0.5741125	36.4220479
GO:0009205	purine ribonucleoside triphosphate metabolic process	0.033742375	0.58476996	41.1791708
GO:0009199	ribonucleoside triphosphate metabolic process	0.034593574	0.58312761	41.9751939
GO:0006091	generation of precursor metabolites and energy	0.03610049	0.58839461	43.3597731
GO:0009144	purine nucleoside triphosphate metabolic process	0.038109124	0.58825354	45.1573304
GO:0009152	purine ribonucleotide biosynthetic process	0.039015563	0.58726975	45.9509181
GO:0055085	transmembrane transport	0.042081945	0.60604395	48.5566327
GO:0009260	ribonucleotide biosynthetic process	0.042750615	0.59362044	49.1090183
GO:0009141	nucleoside triphosphate metabolic process	0.046658895	0.60897427	52.228246

Annotation Cluster 5		Enrichment Score: 1.1516193992206216		
Term		**p-value**	**Benjamini**	**FDR**
GO:0001568	blood vessel development	0.028163983	0.57774561	35.7041482
GO:0001944	vasculature development	0.030823763	0.58598984	38.3715132

Table 4- Analysis of common and unique genes during the first 48 hrs of 3T3-L1 adipogenesis

Comparison	GO biological process complete	Mus musculus - REFLIST (22221)	upload_1 (230)	upload_1 (expected)	upload_1 (over/under)	upload_1 (fold Enrichment)	upload_1 (P-value)
Common to all time points	xenobiotic glucuronidation (GO:0052697)	9	9	0.09	+	96.61	9.70E-12
	flavonoid glucuronidation (GO:0052696)	9	9	0.09	+	96.61	9.70E-12
	flavonoid metabolic process (GO:0009812)	11	9	0.11	+	79.05	5.80E-11
	cellular glucuronidation (GO:0052695)	12	9	0.12	+	72.46	1.26E-10
	uronic acid metabolic process (GO:0006063)	13	9	0.13	+	66.89	2.56E-10
	glucuronate metabolic process (GO:0019585)	13	9	0.13	+	66.89	2.56E-10
	cellular response to xenobiotic stimulus (GO:0071466)	50	10	0.52	+	19.32	1.68E-06
	xenobiotic metabolic process (GO:0006805)	46	9	0.48	+	18.9	1.66E-05
	response to xenobiotic stimulus (GO:0009410)	56	10	0.58	+	17.25	4.95E-06
	monosaccharide metabolic process (GO:0005996)	152	12	1.57	+	7.63	7.67E-04
	single-organism carbohydrate metabolic process (GO:0044723)	301	15	3.12	+	4.81	6.68E-03
	cell adhesion (GO:0007155)	754	35	7.8	+	4.48	1.34E-09
	biological adhesion (GO:0022610)	764	35	7.91	+	4.43	1.95E-09
	carbohydrate metabolic process (GO:0005975)	385	17	3.98	+	4.27	6.36E-03
	cell-cell signaling (GO:0007267)	792	34	8.2	+	4.15	2.62E-08
	nervous system development (GO:0007399)	2086	50	21.59	+	2.32	1.40E-04
	multicellular organism development (GO:0007275)	4498	76	46.56	+	1.63	3.16E-02
	single-organism developmental process (GO:0044767)	5073	85	52.51	+	1.62	8.08E-03
	developmental process (GO:0032502)	5112	85	52.91	+	1.61	1.12E-02
	primary metabolic process (GO:0044238)	7337	113	75.94	+	1.49	2.66E-03
	cellular metabolic process (GO:0044237)	7109	109	73.58	+	1.48	7.04E-03
	organic substance metabolic process (GO:0071704)	7692	117	79.62	+	1.47	2.59E-03
	metabolic process (GO:0008152)	8159	122	84.45	+	1.44	2.85E-03
	single-organism cellular process (GO:0044763)	8646	129	89.49	+	1.44	8.63E-04
	cellular process (GO:0009987)	13696	182	141.76	+	1.28	8.17E-05
	G-protein coupled receptor signaling pathway (GO:0007186)	1803	3	18.66	-	< 0.2	4.79E-02
Unique to 24 hr	negative regulation of response to cytokine stimulus (GO:00607	43	5	0.24	+	21.01	4.10E-02
	DNA repair (GO:0006281)	400	12	2.21	+	5.42	2.22E-02
	cellular response to DNA damage stimulus (GO:0006974)	618	15	3.42	+	4.38	1.60E-02
	cellular macromolecular complex assembly (GO:0034622)	624	15	3.45	+	4.34	1.80E-02
	cellular macromolecule metabolic process (GO:0044260)	5396	60	29.87	+	2.01	2.97E-05
	macromolecule metabolic process (GO:0043170)	6113	66	33.84	+	1.95	7.53E-06
	cellular nitrogen compound metabolic process (GO:0034641)	4081	44	22.59	+	1.95	3.18E-02
	primary metabolic process (GO:0044238)	7337	78	40.61	+	1.92	4.49E-08
	organic substance metabolic process (GO:0071704)	7692	80	42.58	+	1.88	5.30E-08
	nitrogen compound metabolic process (GO:0006807)	6786	69	37.56	+	1.84	3.16E-05
	cellular metabolic process (GO:0044237)	7109	72	39.35	+	1.83	1.07E-05
	metabolic process (GO:0008152)	8159	80	45.16	+	1.77	1.51E-06
	cellular process (GO:0009987)	13696	101	75.81	+	1.33	6.09E-03
Unique to 48 hr	positive regulation of molecular function (GO:0044093)	1317	23	7.88	+	2.92	3.07E-02